THE SYNTHESIS AND CHARACTERIZATION OF GERMANIUM NANOPARTICLES AND NANOWIRES AND THE STUDY OF THEIR POTENTIAL IN PHOTOVOLTAICS

A Thesis

Presented to the Faculty of the Graduate School

of Cornell University

In Partial Fulfillment of the Requirements for the Degree of

Master of Science

by

Stephen Corey Codoluto

August 2009

ABSTRACT

The increasing energy demand of an overpopulated society has bolstered the interest in exploring renewable energy forms, one of which is solar energy. Current solar cell technology is neither an efficient nor cost-effective alternative to currently used fossil fuels. Nanostructured semiconductor building blocks are expected to play a central role in the development of next-generation cost-effective solar cell technology. Among the various materials that have been explored and studied, Ge holds particular promise due to it favorable band gap and good transport characteristic. A method to produce colloidal Ge nanocrystals, however, has not yet been established. Colloidal synthesis provides a scalable and cost-effective route to nanocrystalline semiconductor material as building blocks in low-cost PV energy conversion devices. This work describes the synthesis and characterization of Ge nanoparticles and Ge nanowires and their potential applications. Ge nanoparticles, 1.9 – 16.0 nm, are synthesized via colloidal synthesis by reducing germanium iodide using a strong reducing agent in various coordinating solvents. The effects of reaction and injection temperature, reaction time, and initial concentration are studied. A minimum temperature of 250 °C is required to crystallize Ge in a colloidal synthesis, below which only amorphous material is formed. An increase in reaction temperature from 250 to 300 °C has little effect on the final nanocrystal size and structure. A temperature of 200 °C was found to minimize crystal growth defects. Increasing or decreasing the injection temperature increased the crystal defects. The final crystalline products are analyzed using XRD, FTIR, TEM, HR-TEM, SEM, UV-vis spectroscopy, and PL to study oxidation, crystal structure, and optical properties. Spin coated germanium nanoparticles are combined with sputtered a-Si to create a polysilicon-Ge matrix which could direct charge transfer and decrease recombination of photogenerated charges. As a complementary

nanocrystalline Ge building block nanowires were also synthesized by the thermal decomposition of DPG and TMG in supercritical hexane using a batch and a semi-continuous supercritical reactor. Up to 210 mg are synthesized and collected using this process with a diameter range of 20 nm to 60 nm and lengths up to 15 μm. The continuously grown nanowire experimental yield is ~35%, compared to the batch experimental yield of 15%. The Ge nanowires were easily extracted from the collection vessel and characterized using TEM, SEM, and XRD to confirm the presence of Ge and to study the structure of the wires.

BIOGRAPHICAL SKETCH

Stephen Codoluto was born in New York on December 10th 1984. He received Bachelor of Chemical Engineering and a B.S. in Chemistry degrees from the University of Minnesota-Twin Cities in 2007. He is currently in graduate school working on an M.S. in Chemical Engineering at Cornell and is expected to graduate in 2009.

Every great advance in science has issued from a new audacity of imagination.

John Dewey

ACKNOWLEDGEMENTS

I would like to the National Science Foundation for support of my research. I would also like to thank the facilities provided by KAUST, Cornell Nanofab Facility, and Cornell Center for Materials Research. I would especially like to thank my advisor, Tobias Hanrath, who has helped me develop as a researcher through discussions and constructive criticism, and who has been understanding in more ways than one during my time at Cornell. .

TABLE OF CONTENTS

LIST OF FIGURES

LIST OF TABLES

INTRODUCTION

Motivation

The development and deployment of alternative, renewable energies is becoming an increasingly urgent endeavor for engineers in today's world. Non-renewable fossil fuels comprised of coal, petroleum, and natural gas supply over 80% of the world's energy [1]. The combination of accelerated depletion of a limited resource with the growing concerns about rising CO_2 emissions has opened the pathway for alternative energies. Although renewable energy (i.e. biomass, hydroelectric, solar thermal, photovoltaics) is the fastest growing energy source, its overall contribution to the nation's energy consumption is less than 7%. Photovoltaics, although growing up to 30% annually, still supply less than 1% of that fraction [2]. The solar energy that strikes the Earth's surface is 120,000 TW whereas the current global energy demands 13 TW, providing more than enough energy even if only a small fraction of the sun's energy is harnessed [3]. There are a number of technical and non-technical issues that must be overcome to benefit from the full potential of photovoltaics. The most prominent of these includes the photon conversion efficiency, which is determined by the types of materials, interfaces, and engineering incorporated into the device. Cost and practicality are other factors inherently linked to the efficiency of the cell. The potential for growth in this area and the challenges that need to be overcome make it an ideal candidate to research.

The main challenges with current solar cells are efficiency and cost. Efficiency is defined here as the fraction of sunlight that hits a target cell and is converted to electrical energy. The current cost of electricity from solar cells is ~$0.30/kWh, in contrast to average electricity costs at $0.09/kWh [2]. Renewable energy systems should be:

(1) Cost effective - significant cost reduction via inexpensive materials and processing techniques.

(2) Efficient - increase the fraction of solar spectrum absorbed and converted to useful forms.

(3) Storable - develop energy storage technologies, such as lithium-ion batteries, in conjunction with photon energy harnessing techniques to create a self sustaining energy source.

There are a number of important considerations to take into account when constructing a solar cell such as the fraction of energy that a cell can efficiently absorb and convert into useful energy. An ideal thin film of nanocrystals (NCs) fabricated into a solar cell would have quantum confinement effects and optical properties dependent on the type of nanoparticle. A film of NCs would have optical properties that absorb an average wavelength in the electromagnetic spectrum. NCs that have a given band gap energy, E_g, and absorb IR light, which has about half the energy of UV light, would not be able to effectively convert the UV light simultaneously due to photon excitations. If a photon with energy equivalent to UV light excites an electron-hole pair in a NC that has a lower E_g than the incoming photon energy, the electron will be ejected from the valence band and will lose energy in the form of heat in the cell and subsequent phonon emission, ultimately lowering the efficiency of the device. Ideally an electron would be excited by a photon with energy exactly equal to its E_g which would create an electron-hole pair that could be harnessed in the absence of recombination. Since only a small fraction of incoming photons have energy equal to that of the NC E_g, a multilayer solar cell with varying NC sizes may aid in the ‘capture’ of a range of energies from incoming photons.

Conventional p-n junction solar cells are restricted to a maximum of ~30% efficiency called the Shockley-Queisser limit [4]. The two restrictions that define this efficiency are the inability to absorb light with energy less than the band gap of the material, and the loss of photon energy in excess of the band gap [5].

There are several ways to recover energy above the band gap and increase the efficiency above the Shockley-Queisser limit. The first of which are multijunction cells in which a higher band gap material is typically stacked on top of lower band gap materials to filter out most of the high energy photons (i.e. blue light). The less energetic photons pass to the lower band gap materials (i.e. red and IR). The cells are then connected in series and the energy output is extracted from each material separately and added. A device of this sort with stacked layers would provide a more tunable band gap range for the solar spectrum, but are typically costly to fabricate due to the intricate designs in the interface boundaries. An infinite number of layers, although impossible to theoretically achieve, would have a maximum efficiency of 68% [5]. Ge would provide a low cost option for these types of cells due to their potential in forming thin films via solution processing. Although there are a number of high and intermediate band gap materials on the market (i.e. CdSe, CdS, and PbS) there are few low band gap materials suitable for photovoltaics. Ge, with its low band gap energy, could be used as a bottom layer in a multijunction cell to capture the photons in the IR region.

Another proposed option, although more controversial, is by exploring the strong confinement of photon-electron interactions in nanoscale materials via a process known as multi-exciton generation (MEG). The process of MEG has been proposed as a phenomenon where instead of one photon exciting one electron-hole pair, it could

excite up to seven electron-hole pairs in the material depending on the incident energy and material band gap [6]. In this system, energy above the band gap is converted into multiple carriers in a single junction cell. Ge could potentially be more promising than materials like PbSe since effective masses in Ge are more asymmetric, so the MEG threshold would occur closer to the thermodynamic limit.

The most efficient solar cells on the market are multijunction cells with efficiencies >40% [7]. These are designed to absorb a large range of incoming wavelengths by implementing a series of cascaded junctions with decreasing energy gaps [8], [9]. These cells are comprised of stacks of carefully lattice matched compound semiconductors, like GaAs or GaInP, and Si or Ge, but are expensive to fabricate because they are typically made by molecular beam epitaxy (MBE), a time consuming and instrumentation-intensive technique.

Nanomaterials as building blocks for photovoltaics are being studied for their applications in thin films, tunable energy gap to accommodate a greater portion of the sun's rays, and quantum confinement effects. Bulk Ge and Si have indirect band gaps and photoluminescence occurs in the IR region yielding low efficiencies [10]. As the NC radius is decreased below that of the Bohr radius of the electron-hole pair, the material transitions to a direct band gap and photoluminescence occurs in the visible light region [11]. Group IV semiconducting nanomaterials (e.g.: Si and Ge) are of interest due to their non toxicity, narrow nanoparticle size distribution, stability, and quantum confinement effects. Compared to other non-standard compound semiconductors, the technological application of these group IV materials benefits from an existing vast library of knowledge on their bulk properties and processing.

This will greatly facilitate their assimilation into existing technologies. Ge is particularly interesting because it has more favorable energetic states than Si. The lower band gap energy is better for harvesting infrared (IR) energy. By directing the absorbed photon and electron-hole pair through a specific pathway attainable through nanocrystal arrays, the solar cell theoretical conversion limit can be raised from 30% to 43% [12].

Despite the recognized potential of Ge nanomaterials in photovoltaics, current challenges involve finding a viable, robust, and practical synthesis route. This has been a difficult task due to the reaction chemistries and higher temperatures required for crystallization of group IV semiconductors. In contrast to ionic compound semiconductors which can be crystallized from molecular precursors at lower temperatures (e.g.: PbSe at T~120 ^{o}C) [13], nucleation and growth of nanocrystalline Ge requires much higher temperatures. These higher temperature in addition to overcoming the high energy barrier present in Ge stem from Ge's strong covalent bonds [9], [14], [15], [16]. Solution based synthesis is most desirable, providing a robust method for growing Ge nanocrystals in a controlled manner and results in the highest yields. Alternative methods such as MBE have been used for fundamental studies, but their prohibitive cost make them inappropriate for large scale practices [17], [18].

In addition to their potential in photovoltaics, Ge nanocrystals and nanowires may be promising as building blocks for thermoelectric energy conversion and electrical energy storage. Previous theoretical and experimental work has illustrated the promise of low-dimensional composite structures (e.g. Ge nanocrystals in a $Si_{1-x}Ge_x$ matrix) [19] as transformative thermoelectric material with high thermal resistivity, electrical

conductivity and thermopower. Moreover, Ge nanowires present an attractive candidate anode material for next-generation rechargeable lithium ion battery technology (LIB). In addition to being a much safer alternative to Li anodes, a fully lithiated ($Li_{4.4}Ge$) anode boasts a theoretical charge capacity of 1600 mAh/g – a manifold improvement over the capacity of currently used lithiated graphite anodes (370 mAh/g) [20], [21]. Taken together, these properties provide a strong incentive for the development of Ge nanocrystals as building blocks in next-generation photovoltaic, thermoelectric, and LIB technologies.

Significant previous work

Ge Nanoparticles: A Fine Line between Quality and Quantity

Due in large part to their unique optoelectronic properties, and more pronounced quantum confinement effects than Si, Ge nanomaterials have attracted attention in the last decade due to their promising effects as a type IV semiconducting material. The two major challenges with Ge are attaining high synthesis yields and robust control over interfacial chemistry. Studies in bulk systems revealed that the Ge/GeO_x presents a much more complex interface challenge compared to Si/SiO_x, however, a number of wet and vacuum chemistries have been developed to study, passivate, and functionalize Ge surfaces [22].

Past methods to synthesize high quality Ge NCs have been molecular beam epitaxy (MBE) and supercritical (SC) reactions. MBE is a research oriented technology [23] whereas SC reactions provide low yields, but have a potential for large scale processes

due to the system's applicability towards a continuous flow through system [24]. An alternative method for synthesizing Ge is a colloidal-based process that is capable of providing larger quantities of Ge nanomaterials but with poor control over size and shape, thus exemplifying the balance between quality and quantity. Because the particle sizes cannot be as carefully controlled, the quality of the particles is lower than MBE grown particles. The two modes of solution syntheses that have been studied are (1) thermal degradation of organogermane precursors, [10], [16], [17], [25], [26] and (2) reduction of germanium halide salts [24], [27], [28], [29]. In the case of thermal degradation, an organogermane precursor such as tetraethylgermane or diphenylgermane is reacted by heating the precursor to its decomposition temperature. This reaction is simple and high quality particles are formed; however, high reaction temperatures are required [25]. The second method uses a chemical reaction involving germanium halide and a strong reducing agent. The complexity of these reactions and their numerous reactants increase the variable reaction parameters which precludes rigorous control over nucleation and growth and result in larger particle size distributions [10], [30].

Higher yield is desired for practical and scaling aspects, but particle crystallinity and size distribution are also important. Uniform particle sizes are important for two key reasons. First, to allow the particles to assemble into well-ordered arrays, which facilitate efficient charge transfer and minimize charge recombination. Secondly, effective size control is imperative to successfully map the particles size dependent properties such as optical characteristics and interparticle surface interactions [31], [32].

Ge Nanowire Growth

Ge nanowires have also been extensively studied since they have an inherent quantum confinement effect similar to Ge nanoparticles, but have an unconstrained dimension (*i.e.,* the nanowire access) for electrical access [33]. Nanowires may be beneficial in photovoltaic devices, since they can be incorporated into a device with nanoparticles to reduce the interparticle electron transport interactions. The nanoparticles would harvest the photon while the nanowire would facilitate fast and efficient charge transfer. Specifically, the Ge nanowires would allow a continuous crystalline pathway for high mobility transport of photogenerated charges. Moreover, Ge nanowires also hold promise as anode materials in lithium ion batteries since their one-dimensional shape can accommodate the large volume dilations (400%) accompanying de-lithiation cycles through radial expansion while preserving electrical conductivity along the nanowire axis [20].

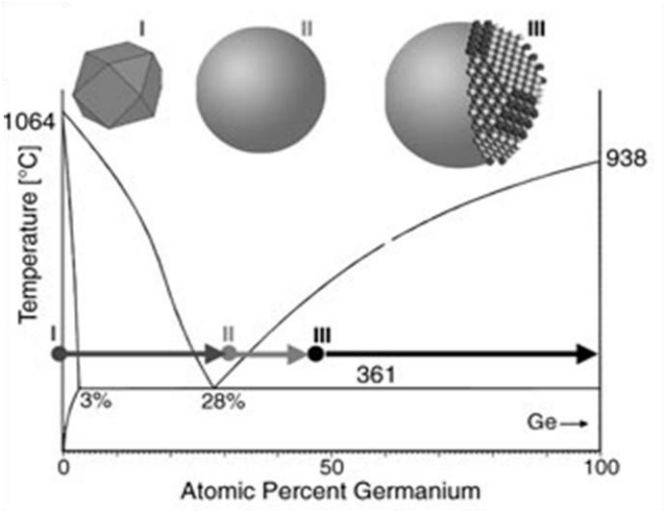

Figure 1: Phase diagram for Ge wire growth from Au seed taken from ref. [1].

Contrary to the homogeneous nucleation mechanism at the heart of Ge NC synthesis discussed above, Ge nanowires are formed via heterogeneous nucleation in a process known as the vapor-liquid-solid (VLS) mechanism. The semiconductor precursor is degraded in the presence of a colloidal metal nanoparticle which acts as a seed for the one dimensional crystallization and directs the growth of highly anisotropic single crystal wires.

Details of the VLS growth mechanism are shown in Figure 1. Briefly, the nanowire nucleation and growth in a SC environment involves three distinct regions; I) The Au nanoparticle forms an alloy with the Ge as the solution is heated. II) As the Ge concentration is increased, the alloy droplet liquefies, and eventually III) Ge supersaturation induces crystallization on the droplet surface [34], [35]. Other seeding materials have also been studied including Ni and Bi which can change the growth orientation or growth rate [36]. The diffusion rate and the process of forming an alloy droplet due to different seed:Ge eutectic temperatures can also be affected by the type of seed particle [37]. The high strength and flexibility of single crystal Ge nanowires would be beneficial for flexible devices and practical integration into device substrates [38].

Studies have also been done to understand the stability of nanoparticles and nanowires and how passivating these surfaces reduce oxidation. The types of passivating agents that are typically used involve hydride, sulfide, chloride, or alkyl linkages to the particle or wire surface, thus protecting it from oxidizing [22]. These ligands can vary in length and may provide unique advantages such as solubility, stability, and feasibility of device integration.

Device Integration

Beyond synthesizing Ge nanomaterials for their fundamental properties the major driving force behind fabricating them is the promising application of their properties in technological devices. Ge is unique in that it works as a photodetector in the mid to near infrared region [39]. Although half of the sun's energy reaching the earth is beyond 700 nm, current photovoltaic devices do not absorb this significant range of the solar spectrum. In photovoltaics size controlled properties can be exploited to optimally match the absorption of the active layer to the emission of the solar spectrum. Size control is also important in LED devices because particles below their Bohr radius lead to radiative recombination [10], [40]. Quantum confinement allows a tunable band gap for Ge from the IR to the near visible. These factors make Ge a promising candidate for future photovoltaics with efficient harvesting in the IR region.

Incorporation of Ge into the active layer of prototype photovoltaic cells presents conflicting challenges that must be balanced to maximize efficiency. The thicker the active layer of the photovoltaic device the more incident light is adsorbed, but it also must be thin enough to efficiently collect the photogenerated charges. Vertical particle alignment, dependent on particle size distribution and surface chemistry, is important for electron channeling to occur more readily which may be improved by using nanowires. Closer interparticle contact is another parameter that should be considered as once the electron-hole pair is generated the particles must be close enough to allow the charge to hop from particle to particle.

The next step after synthesizing and characterizing the nanomaterials is to manufacture them for commercial use. There are four feasible proposed applications that Ge nanomaterials could be applied; PV single junction cells, PV multiple junction cells, encapsulated nanostructures which are important for PV and thermoelectric applications, and applications for electrical energy storage. The simplest of designs would involve a single junction cell that would use a thin film of Ge as the active layer. The second device, as discussed above, is a multijunction solar cell that would integrate Ge into its configuration, with the restriction that MBE-based fabrication is prohibitively expensive. Another proposed application of Ge is incorporating it in a nanocrystal heterojunction. These devices would involve Ge nanoparticle arrays in a percolated polysilicon matrix. In this configuration, the large interfacial area could be tailored to reduce charge recombination.

Any of the above three discussed application could then be paired with an energy storage system. This combined system would harness energy in the PV part followed by the efficient storage for later use in the second part, ultimately creating a self charging battery. Although the current photovoltaic devices are some of the most efficient cells an innovative next generation technology must be developed for photovoltaics to be seriously considered as an alternative energy [41], [42]. It should be noted that the progress in each of these applications is dependent upon the successful synthesis of Ge nanomaterial building blocks. The present work investigated solution and supercritical fluid synthesis approaches to Ge nanomaterials with controlled shape, size and surface chemistry

MATERIALS AND METHODS

Synthesis of Ge nanocrystals

All reactions were performed with as received germanium (II) iodide (GeI_2, purity 99.99%, Aldrich) as a precursor and the strong reducing agent, 1.7-3.2 M tert-butyllithium in heptane (t-butLi, Aldrich), with the exception of the reaction run with lithium aluminum hydride ($LiAlH_4$, Aldrich) used as a weaker reducing agent for comparison. It should be noted that caution should be exercised when handling these reducing agents as they are extremely pyrophoric. These reagents were handled under a strict Nitrogen environment with the exception of transferring them to the reaction flask which was done by a syringe in an air tight bag. As received hexadecylamine (HDA, purity 90%, Aldrich) was distilled under vacuum at ~250 °C. The distillate was immediately stored under nitrogen. The distilled HDA did not show any noticeable effects in the reaction products when compared to the as received HDA. Trioctylphosphine (TOP, purity 99%, Aldrich), squalene (purity 98%, Aldrich), dodecanethiol (purity 99%, Aldrich), and octadecene (ODE, purity ≥ 95%, Aldrich) were used as received. TOP was distilled under vacuum but the 'purified' distillate did not affect the product yield or crystal structure in any noticeable factor.

The colloidal synthesis methods were performed in a 50 mL round bottom flask connected to a Schlenk line. The experimental system was evacuated for 10 min followed by a gentle flow of nitrogen 15 min prior to the introduction of any reactants. The reaction was maintained in a positive nitrogen environment throughout the course. Once the system was purged with N_2, 0.30 – 0.50 g of GeI_2 was dissolved in 10 - 15 mL of each solvent, which was prepared in a nitrogen glove box, and then injected through a syringe into the flask. The solution was heated to the injection temperatures of 120 °C, 150 °C, or 200 °C for each reaction, at which point the coordinating solvent

(if different from the initial solvent) was introduced into the system followed immediately by a quick injection of t-butLi through a syringe. The contents of the flask were stirred vigorously and heated to the reaction temperatures of 250 °C or 300 °C for each reaction over 7 min. The temperature was controlled to within ± 3.5 °C for the duration of the reaction using a thermocouple and a process controller. Each reaction was run at lengths of 45 min, 60 min, or 120 min. Shorter reaction times did not yield reproducible results.

Once the reaction time was complete the contents of the flask were allowed to cool to 30 °C, with the exception of reactions with HDA which were allowed to cool to ~80 °C. To recover the nanocrystals and separate the product from the supernatant solution, 10 mL of methanol anti-solvent was added to the solution and the solution was centrifuged for 10 min at 3750 rpm. The precipitate was redispersed in 10 mL of chloroform followed by the addition of 10 mL of methanol to precipitate the particles but retain the impurities in the liquid phase. The solution was then centrifuged for 5 min at 3750 rpm. This washing and centrifuging process was repeated until impurities could not be seen via XRD analysis and showed only Ge crystalline peaks.

The Ge NCs were characterized using a FEI Tecnai T-12 transmission electron microscope (120 kV), a FEI Tecnai F-20 transmission electron microscope (300kV), and a LEO 1550 FESEM (Keck SEM) for imaging. Crystal and structural analyses were done using a scintag theta-theta Pad-X X-ray diffractometer and an OMNIC FTIR. Optical properties were studied using a shimadzu UV-3101PC UV-vis/near-IR spectrophotometer.

Synthesis of Au nanoparticles

Au nanoparticles were synthesized as a nucleation site for Ge nanowire synthesis [43]. 0.558 g of tetra-n-octylammonium bromide ($(C_8H_{17})_4NBr$, purity 98%, Aldrich) was mixed with 6.94 mL of chloroform (purity ≥ 99% anhydrous, Aldrich) to make solution 1. 0.077 g of gold chloride (III) trihydrate ($HAuCl_4 \cdot 3H_2O$, purity ≥ 99.5%, Aldrich) was mixed with 7.5 mL of distilled water to make solution 2. 50 µL of 1-dodecanethiol (purity 99%, Aldrich) and 0.099 g of sodium borohydride ($NaBH_4$, purity ≥ 98.5%, Aldrich) were added to 6.25 mL of distilled water to form solution 3. Solution 1 was added to solution 2 in a 20 mL container and stirred vigorously for 1 hr. The bottom organic phase containing the Au precursor was extracted from the solution and slowly added to solution 3. The contents were stirred for 14 hrs at which point 7.5 mL of ethanol was added to the solution to precipitate the Au nanoparticles. The final solution was centrifuged for 5 min at 10000 rpm and the precipitate was retained. The particles were re-dispersed in chloroform and precipitated with ethanol to repeatedly clean the particles of any reaction impurities while at the same time performed size selective precipitation.

Supercritical synthesis of Ge nanowires

N-hexane (sure seal, purity ≥ 99% anhydrous, Aldrich), diphenylgermane (DPG, purity 99%, Gelest) and trimethylgermane (TMG, 99%, Gelest) were used as received in the supercritical (SC) syntheses. A diamond cut piece of Si (100) wafer (7mm x 50 mm) was placed inside the reactor chamber to help collect the nanowires during the reaction. The wafers were cleaned by sonicating in acetone for 30 min, rinsed with 2-

proponal, and finally dried rapidly with an air stream. The cleaned wafer was inserted into a 10 mL volume reactor chamber shown in Figure 2 below.

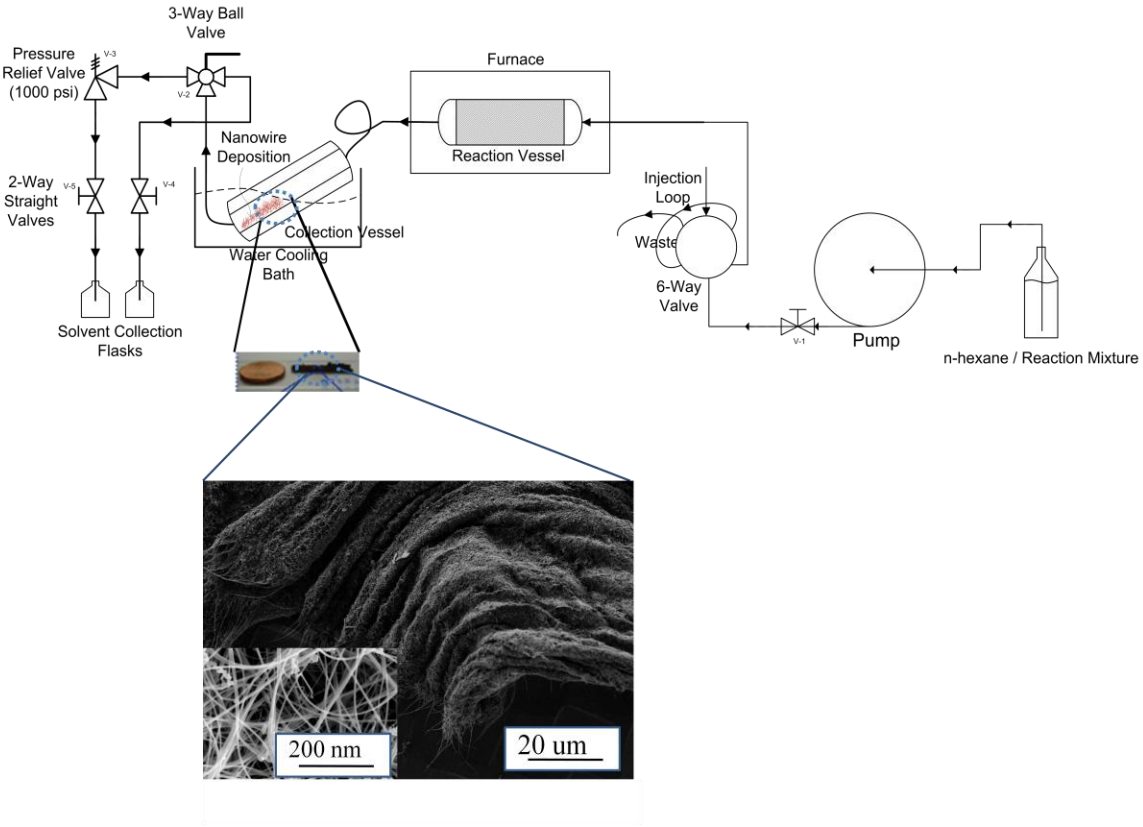

Figure 2: Supercritical reactor design for batch and continuous process to grow Ge nanowires.

The system was rated to 10,000 psi and 400 °C. All components of the pressure system were purchased from High Pressure Equipment. A 10,000 psi rated Varion Prostar 210 pump was used to pressurize the system. Once the wafer was placed in the reactor the system was sealed and pressurized to 500 – 2000 psi. Prior to synthesis, the supercritical fluid reactor was pressure tested to ensure a leak rate of ≤ 1 psi/sec. The reactor was then heated by a circular furnace that provided three sections of adjustable but uniform heat supply. The reactor was allowed ample time to reach a steady state. The reactor was designed to facilitate a batch and continuous process. 200 mM of

DPG or TMG in n-hexane precursor solution was prepared under nitrogen. A solution of Au nanocrystals was added to the germanium precursor solution to achieve a Au:Ge molar ratio of 1:1200 for all reactions except those involving Au:Ge ratio studies.

Supercritical synthesis of Ge NWs in a batch process

The Ge-Au precursor solution was transferred to a syringe and rinsed through the injection loop prior to injection into the reactor. The 3 mL injection loop was then filled with the Ge-Au solution and the contents were quickly injected into the reactor chamber. The driving force by which the precursor solution was injected into the reactor chamber was due to the pressure differential. The system was pressurized using the pump to the desired reaction pressure. Supercritical Ge NCs were also synthesized using this method. The reactor was heated to 450 °C under 2000 psi with a reaction time of 10 min. The stock solution consisted of 200 mM DPG in hexane in absence of Au NCs seed particles.

Supercritical synthesis of Ge NWs in a continuous process

The Ge-Au precursor solution was placed in a small vial with a rubber septum. The vial was attached to the inlet of the pump and pumped through the reactor at a constant inlet flow rate. The pressure in the system was controlled by a pressure control valve at the outlet of the system. For both processes the reaction was allowed to run anywhere from 6 to 40 min. The chamber was cooled to room temperature over 10 min and flushed with n-hexane for at least 15 min. A large fraction or the nanowires were collected as they completed their residence time through the reactor. The remaining nanowires that were deposited in the collection vessel could be collected by

two different methods. The first method depressurized the system rapidly to flush the remaining nanowires out of the system. The second method involved disassembling the collection vessel and collecting the nanowire that way. In both cases the nanowire product yield was ~30-40%.

Optical and crystallographic characterization

The average nanoparticle size was calculated using a measurement of a large sample of particles in TEM images as well as verifying the average size with the Scherrer equation in Eq. 1, where t is the thickness or the NC diameter, 2θ is measured during the scan, and λ and B are constant that are known from the slit width and equipment.

$$t = 0.9\,\lambda/(B\cos\theta) \qquad \text{Eq. 1}$$

Tauc plots were made using the absorbance that was measured by UV-vis spectroscopy. The wavelength was converted to eV and plotted against the molar absorption coefficient. The molar absorption coefficient, ε, was calculated by Eq. 2, where A is the absorbance, d is the sample width, 5 mm, and c was the concentration of solution.

$$A = -\varepsilon * d * c \qquad \text{Eq. 2}$$

The slopes of the plotted data were an indication of the band gap of the material. A Tauc plot defines the optical gap in an amorphous semiconductor [44]. Since Ge is an indirect band gap material in the bulk, the optical gap is an important indication of whether Ge transitions to a direct band gap material with small enough NC sizes or remains as an indirect band material. The product yield of a reaction is defined as the mass of actual Ge nanomaterial divided by the theoretical mass of Ge that is expected is all of Ge in the precursor was converted to Ge NCs.

RESULTS AND DISCUSSION

Ge nanocrystals

There were a wide range of synthesis methods and surface properties pertaining to Ge NCs that were explored during this study. For this reason, the studies of Ge NC growth paired with the underlying question regarding why that path was explored will be presented in the following manner:

1. Exploration of Ge NC synthesis conditions, studying mainly coordinating solvent and practicality in terms of reaction conditions. The question here was to discover which synthesis approach was best suited to provide high quality Ge NCs in technologically significant quantities?
2. Synthesis optimization, including studies on injection and synthesis temperature, reaction time, and reactant concentrations. These were done to answer how the synthesis parameters can be optimized to yield size-controlled Ge NCs?
3. Investigation of Ge NC surface chemistry and related high resolution crystallography. This was done to answer the questions of, what is the Ge NC surface termination and how does the termination relate to the stability, processing and optical properties of the NC? An understanding of these questions would further lead to studies where NCs would be applied with established surface chemistry treatments to modify NC surface chemistry and thus gain control over surface and bulk properties.
4. Optical NC properties were measured to see if the Ge NCs exhibited size dependent optical properties. Specifically, is the photoluminescence due to surface states or an inherent property of the Ge core?

These areas were studied to fully map out the optimal conditions to synthesize Ge NCs as well as to better understand how Ge NCs will behave in photovoltaic devices. A knowledge base of the fundamental optical and structural properties is important in designing and engineering solar cells.

1) *Exploration of Ge NC synthesis, studying mainly coordinating solvent and practicality*

There were several reaction schemes that were explored shown below in Table 1.

Table 2: Experimental reactions showing the solvent, coordinating ligand, and reducing agent used for each Ge NC synthesis.

Reaction	Solvent	Coordinating Solvent	Reducing Agent
A	TOP (15 mL)	TOP	$LiAlH_4$
B	TOP (15 mL)	TOP	t-butLi
C	HDA (10 mL)	HDA	t-butLi
E	HDA (6 mL)	ODE (6 mL)	t-butLi
F	TOP (10 mL)	ODE (1:15 ODE:TOP)	t-butLi
G	Squalene (10 mL)	Dodecanethiol (1 mL)	t-butLi
H	Supercritical hexane	(TMG, DPG 1 mL)	thermal reduction

Initial synthesis efforts focused on Ge NCs in pure TOP using $LiAlH_4$ as a reducing agent at 300 °C [30]. The purpose of this reaction was to determine if TOP would be a suitable coordinating solvent for other NC materials. This reaction, however, produced low yield, low quality particles. The synthesis was successful 1 out of 6 times with the

unsuccessful reactions yielding only amorphous products. The incomplete reduction of the germanium halide precursor was attributed to either a low solubility of the reducing agent in TOP or more unlikely, the low 'oxidation potential' of $LiAlH_4$. A low solubility would lead to a lack of reducing agent during the nucleation injection which would result in only a small fraction of NCs and the rest would result in amorphous Another possibility is that there may have been degradation of the reducing agent over time due to moisture. Ge or unreacted GeI_2. Colloidal NC synthesis requires a homogeneous reaction environment; limited solubility of the reducing agent is unfavorable in this regard. TEM images of this reaction are shown in Figure 3-A along with the XRD of a synthesis yielding crystalline products and of a synthesis run at the same conditions yielding primarily amorphous products.

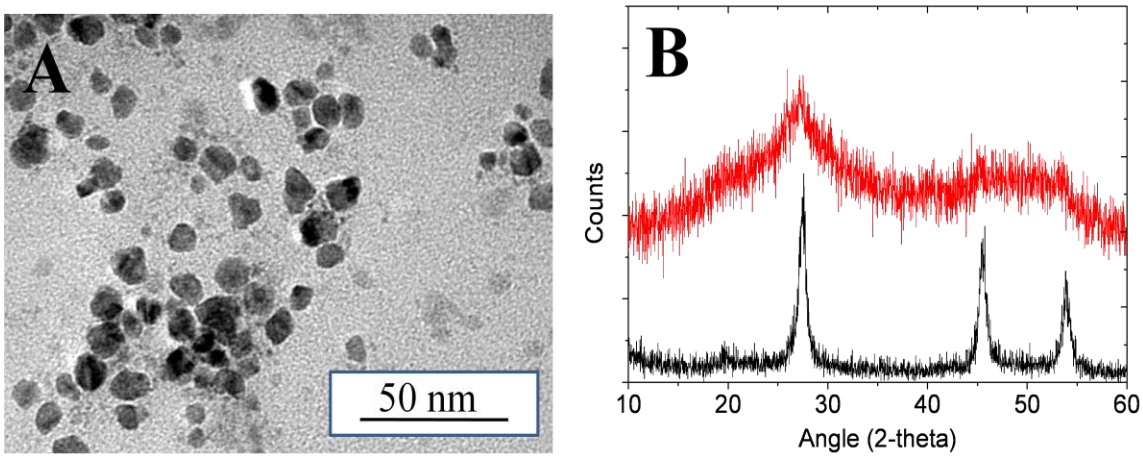

Figure 3: A) TEM images Ge NCs grown in pure TOP at 300 °C for 1 hr using $LiAlH_4$ B) XRD corresponding to TEM images in A) of a synthesis yielding crystalline products (bottom) and of a synthesis run at the same conditions yielding primarily amorphous products (top).

To gain a better understanding of the significance of the reducing agent, we investigated the synthesis based on TOP as the coordinating solvent and an alternative liquid reducing agent, t-butLi. The Ge NCs grown via this method had higher yields and were of a better quality (i.e. better size distribution and crystal shape) than NCs grown using $LiAlH_4$. This method produced NCs that were resistant to oxidation up to 5 hours in air, after which about approximately a quarter of the sample was oxidized. This oxidation was roughly measured with XRD and by massing the remaining Ge NCs after the removal of the GeO_x by centrifucation in toluene. Compared to the reaction with $LiAlH_4$, this reaction had a smaller fraction of oxidized NCs at a certain time exposed to air, but not by a significant amount. This reaction was reproducible, producing the same quality Ge NCs every time. The same reaction was repeated 3 times yielding NCs with an average sizes ranging from 11.4 ± 2.3 nm to 12.2 ± 3.0 nm. This method provided effective size tunability, but HR-TEM images, discussed in a later section, showed that there were numerous twinning defects in the crystal structure. The challenge of rapid growth in addition to inhomogenities at a nanomaterial scale could lead to a polydisperse product (i.e. large NC diameter distribution). The TEM and XRD images are shown in Figure 4, as well as the EDX in Figure 4-C to verify the elements present.

All histograms were made with Image J and Origin. The variable d, o, and n represent average particle diameter, the standard deviation, and the number of particles counted, respectively. The size distribution was fitted with a log-normal function.

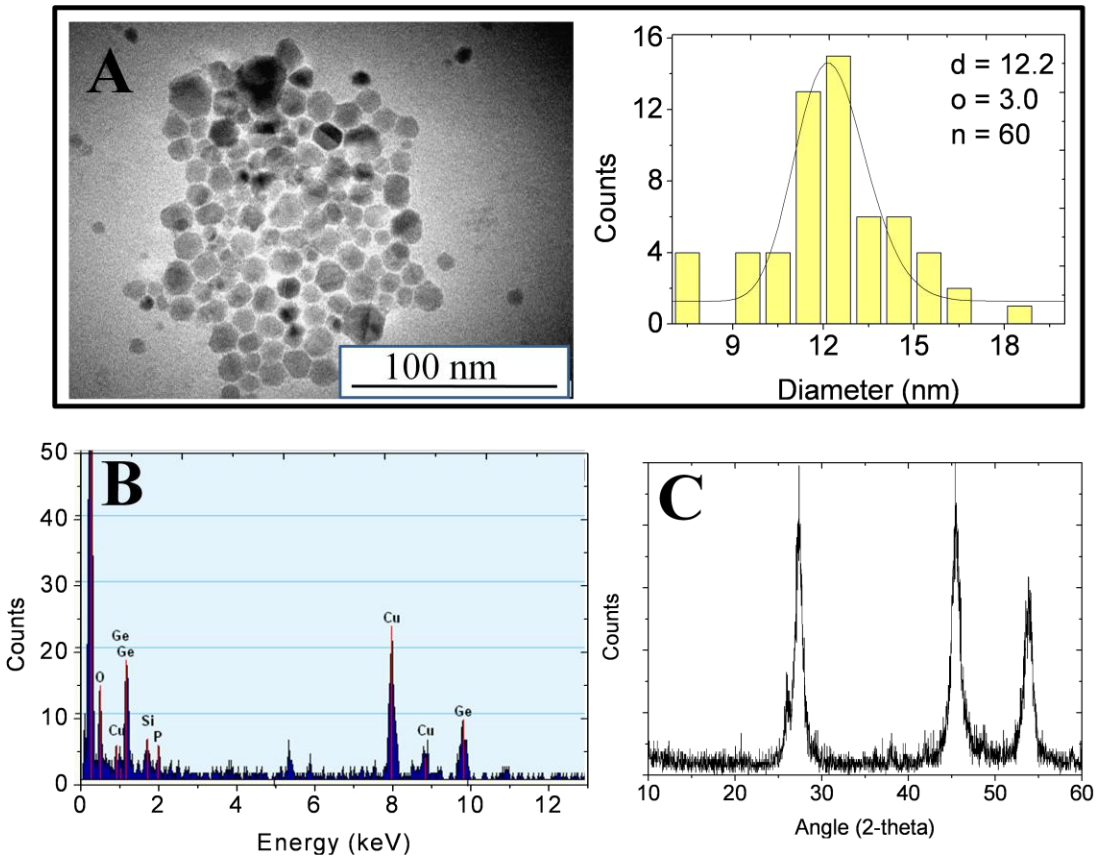

Figure 4: Ge NCs grown in TOP at 300 °C for 1 hr using t-butLi A) TEM image and histogram B) EDX C) XRD.

Whereas TOP is a well established coordinating solvent for compound semiconductor NCs, its role in Ge NC surface termination is poorly understood. Since surface passivation is critical in controlling many facets of NC properties, we explored Ge NC synthesis with alternative coordinating solvents. The work with HDA and ODE described below was inspired by successful demonstration of amine and alkene passivation of bulk Ge surfaces. HDA was explored as a solvent to better control the growth of the Ge nanoparticles. HDA was explored as a candidate for control of growth because it was predicted that the functional group would have an affinity to the

Ge surface while still allowing high temperature synthesis [45]. A functional group with an affinity for the nanoparticle surface coupled with a high boiling point, are two important factors when choosing a coordinating solvent for Ge.

It was hypothesized that HDA would slow the growth rate relative to the TOP reactions. To test this hypothesis, Ge NCs were grown in pure HDA at 300 °C using t-butLi as a reducing agent. This reaction was promising because it produced low defect NCs at high yields. However, the NCs oxidized readily immediately after the reaction was exposed to air indicative of poor surface stability or lack of NC surface coverage. The reaction with pure HDA was also analyzed using low resolution TEM in Figure 5-A, with the corresponding EDX to verify the presence of Ge in Figure 5-C, and XRD depicted in Figure 5-D (top). Compared to the Ge NC synthesis in TOP, reactions in HDA slowed NC growth as well as provided a more uniform size distiribution with a lower number of defects verified by HR-TEM. Both syntheses roughly had the same product yield.

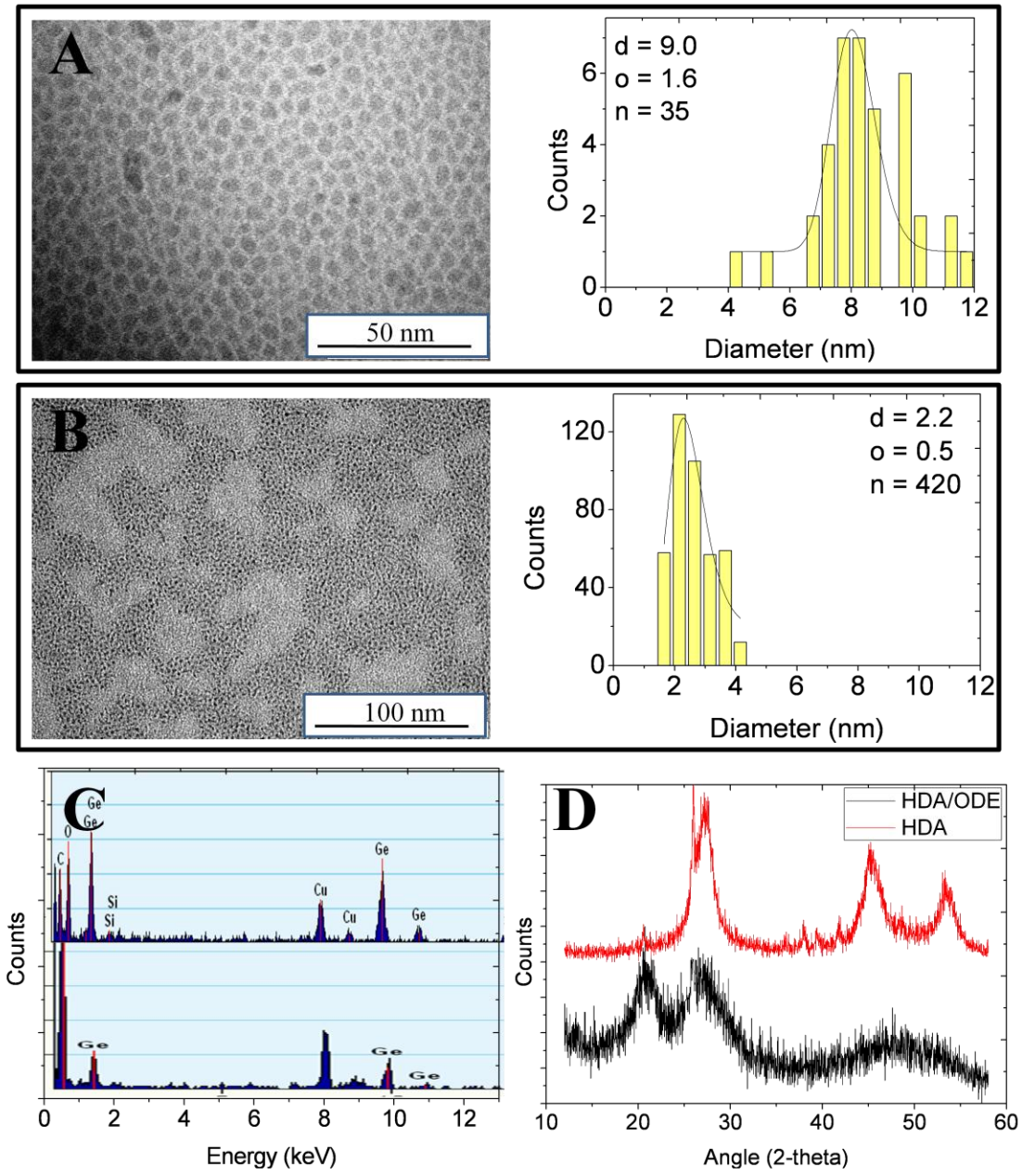

Figure 5: A) TEM image and histogram of Ge NCs grown in pure HDA at 300 °C for 1 hr B) TEM image and histogram of Ge NCs grown in an equal volume mixture of HDA/ODE at 300 °C for 1 hr C) EDX of A) (top) and B) (bottom), D) XRD of Ge NCs grown in pure HDA (top) and HDA/ODE (bottom) at 300 °C and 1 hr.

To address the oxidation concerns with HDA coated Ge NCs, subsequent experiments included ODE as a co-solvent and surface passivating agent. This coordinating solvent was explored due to the higher binding strength of alkenes to Ge than amines [46]. A higher binding strength than HDA was predicted to provide better surface coverage where the NC was completely passivated and the ligand would be difficult to remove. Using an equal volume mixture of HDA and ODE, since NCs have a very low solubility in ODE alone, oxygen resistant Ge NCs were grown. Using ODE not only slowed the growth rate, but resulted in a more uniform size distribution. This reaction, however, was irreproducible and involved an intensive washing process. The NCs were often washed 6 – 8 times before the impurities in the XRD and TEM were minimized. The size of particles, although uniform, were also not reproducibly grown, with the same reaction yielding 2.6 ± 0.5 nm to 4.0 ± 1.4 nm particles.

The reaction products obtained with HDA and ODE were analyzed using low resolution TEM shown in Figure 5-B, with corresponding EDX to verify elemental composition in Figure 5-C, and XRD depicted in Figure 5-D (bottom). The XRD image of NCs grown in ODE and HDA with sizes 2.2 ± 0.5 nm, were at the edge of the diffractometer's range making it difficult to distinguish the nanocrystal peaks. It should also be noted that the broad peak at ~22 degrees was present in all samples and was thought to be due either to the carbon ligand or unwashed impurities remaining in the sample.

The next two reactions were done by reducing GeI_2 at 300 °C with t-butLi. The first of these reactions explored ODE as a co-solvent in the presence of TOP as the main solvent. Ge NCs cannot be grown in pure ODE because the solubility of GeI_2 is too low in ODE even at 300 °C. Without the GeI_2 present in solution the initial nucleation

event that typically causes the Ge NCs to precipitate and grow by Ostwald ripening would not occur efficiently resulting in unreacted and amorphous material. GeI_2 in 1 mL of TOP provided the needed solubility, but the ODE hindered NC growth as is shown in Figure 6-B, resulting in a poor size distribution and misshapen particles. A similar affect with misshapen NCs was also seen in the reaction with HDA and ODE. When the ODE:HDA ratio was greater than 10:5 mL the NC yield decreases significantly and the quality of the NCs decreased. This could indicate that although ODE provides a complete surface coverage and slows growth, and abundance of ODE may either slow growth too much or hinder the growth of the NC to effectively grow high quality crystals.

In a complementary experiment, Ge was grown in squalene with 1-dodecanethiol as a coordinating solvent. This reaction was done to provide a comparison of a Ge NC with a Ge-S ligand to ones with Ge-C and Ge-N linkages. The product yield (~10%) in this synthesis was low and XRD could not be performed. The low yield made this reaction impractical and the reaction was not studied further. TEM images corresponding to these particles are shown in Figure 6-A. It is predicted that the reaction did not work due to the solvent, squalene. The low solubility of GeI_2 in squalene may have attributed to inhomogenties in the solution which would have hindered.

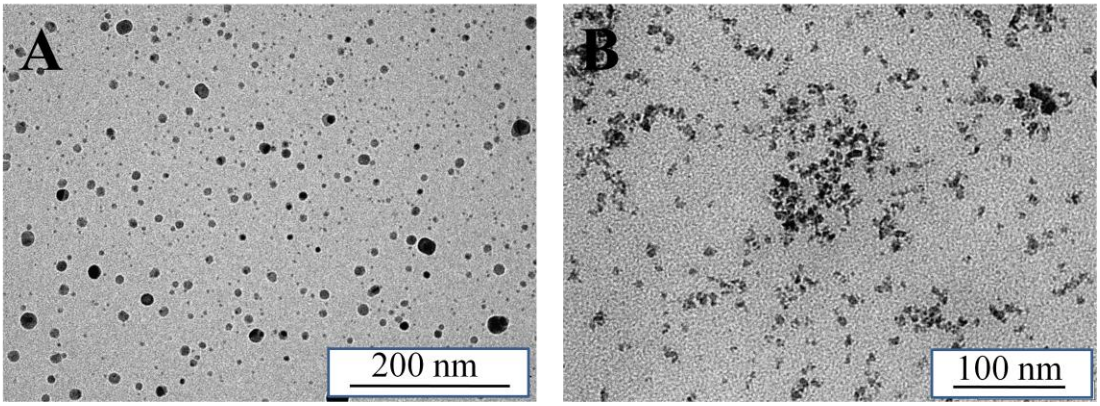

Figure 6: A) TEM images of Ge NCs synthesized in squalene with 1-dodecanethiol at 300 °C for 1 hr, B) Ge NCs synthesized in 15:1 volume mixture of ODE:TOP at 300 °C for 1 hr.

From these seven reaction methods, Ge NCs grown in pure TOP and Ge NCs grown in HDA/ODE using t-butLi yielded the most promising results for further research. The yields were high in both reactions and the final product was highly crystalline. The issue that still needs to be overcome with Ge NCs grown in pure TOP is the oxidation that occurs shortly after air exposure. This could be remedied by a ligand exchange which is currently being studied. The main issue with Ge NCs grown in HDA/ODE solution is the irreproducible cleaning process after the reaction. A possible solution to this problem that has been attempted is trying the washing process with a variety of solvents and anti-solvents. Although this solution has been ineffective so far, it is still being investigated. Once these challenges are overcome the Ge NCs from these reactions would be ideal for studying their electrical properties and subsequent processing in photovoltaic devices.

2) *Synthesis optimization, including studies on injection and synthesis temperature, reaction time, and reactant concentrations.*

The temperature, initial GeI_2 concentration, and reaction time were studied using Ge NCs grown in pure TOP and Ge NCs grown in pure HDA using t-butLi as a reducing agent. It was found that reaction temperature did not have a noticeable effect on Ge NC growth. A temperature of 250 °C was found to be the minimum temperature at which NCs would form, below which would result in only amorphous material. Figure 7 shows the effects of changing the reaction temperature on the NC quality and average size. Increasing the temperature from 240 to 300 °C increased the particle size slightly as indicated by XRD and TEM. This was thought to be due to the higher mobility and an increase in the rate at which Ostwald ripening occurs. Higher temperatures could not be attempted due to solvent boiling point limitations.

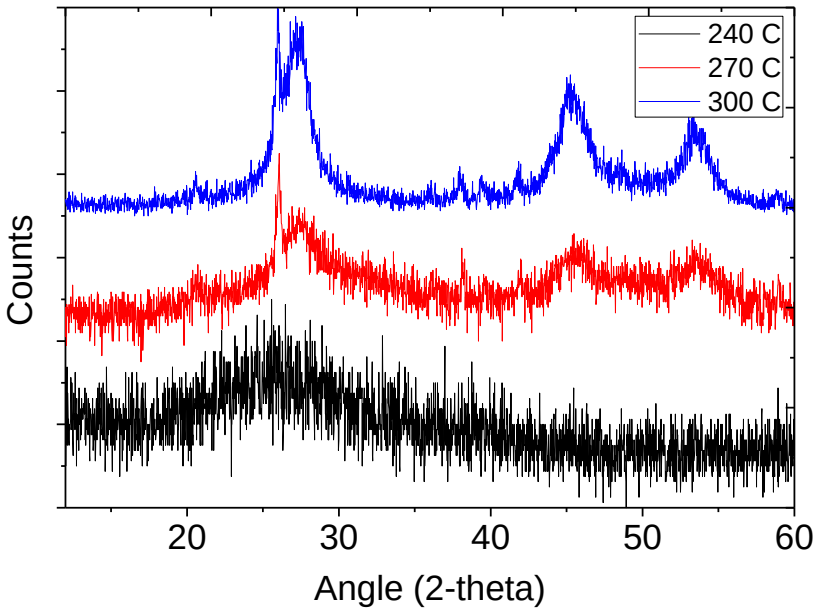

Figure 7: XRD showing the effects of temperature on Ge NCs grown in HDA for 1 hr at (top to bottom) 300 °C (8.2 nm), 270 °C (6.2 nm), and 240 °C.

Changing the injection temperature was found to have little effect on NC growth so long as the temperature was below 200 °C. The same quality NCs were grown at injection temperatures of 100 °C, 120 °C, 150 °C and 200 °C. Injection temperatures above 200 °C produced low product yields most likely due to the extreme reactivity and fast evaporation of the t-butLi. Since the solution was injected above the liquid solution in the vapor region, if the vapor temperature was high enough the t-butLi solution would have evaporated before reaching the liquid phase. There was a noticeable increase in product yield at higher injection temperatures. Injection temperatures of 100 °C, 120 °C and 200 °C resulted in 45%, 70%, and 75% average product yields.

The next variable studied was the initial concentration of GeI_2 and Ge:t-butLi molar ratio in the precursor solution. An increase in precursor concentration from 30.6 mM to 153.1 mM at a constant temperature, resulted in slightly lower yields (70% to 60%) as well as lower quality NCs. Beyond 153 mM Ge NCs were not reproducibly formed often resulting in amorphous material. Since the amount of t-butLi was the same for all three reactions the formation of amorphous material was likely due to a shortage of the reducing agent leading to an incomplete reduction. Figure 8 and Figure 9 show TEM images of GeI_2 grown in HDA and TOP, respectively, at different concentrations. As the concentration was increased, the average particle size increased for both reactions.

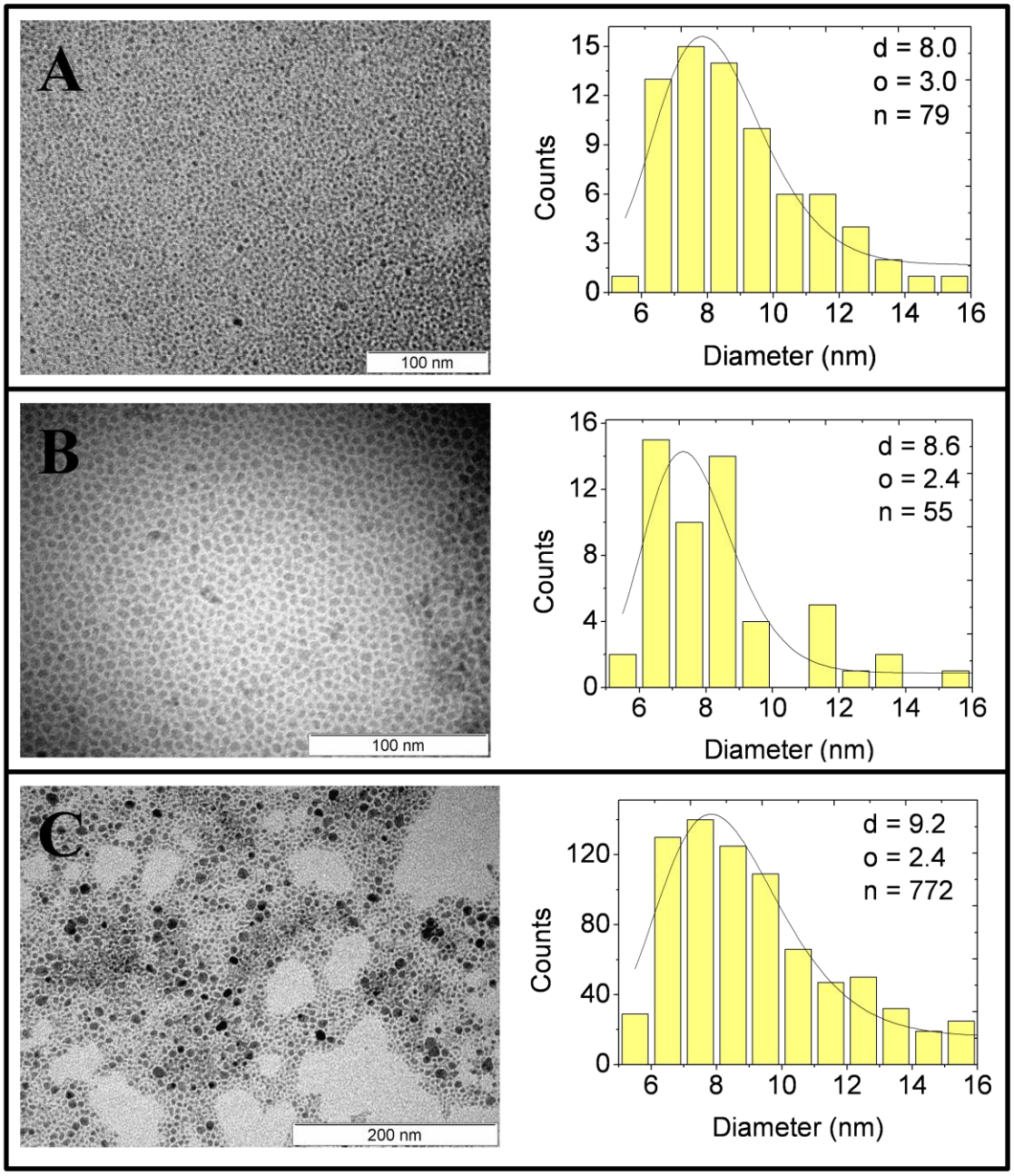

Figure 8: TEM images if Ge NCs grown in pure HDA at 300 °C for 1 hr with an initial concentration of A) 30.6 mM (8.0 ± 3.0 nm), B) 122.5 mM (8.6 ± 2.4 nm), and C) 153.1 mM (9.2 ± 2.4 nm).

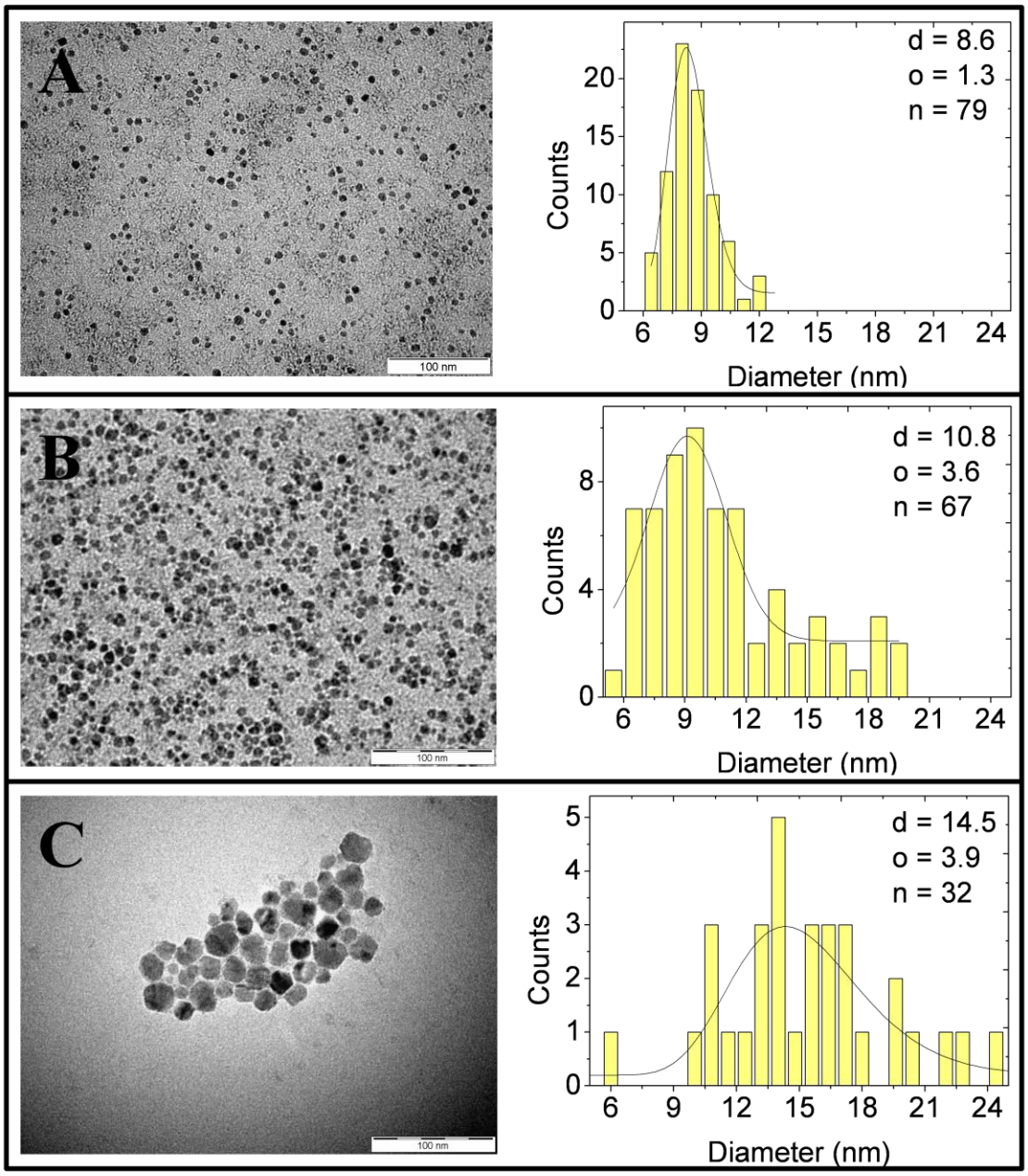

Figure 9: Ge NCs grown in pure TOP at 300 °C for 45 min with an initial concentration of A) 40.8 mM (8.6 ± 1.3 nm), B) 81.7 mM (10.8 ± 3.6 nm), and C) 102.1 mM (14.5 ± 3.9 nm).

An explanation of the degradation of NCs may be a direct effect of Ostwald ripening that occurs during NC growth. In a more dilute solution the particle-particle interactions occur with less frequency than a more concentrated solution. The lower occurrence of interactions might result in a more uniform growth. At higher concentrations the NC growth may be hindered by an abundance of particles collisions and interactions resulting in an increase in crystal growth defects and particle surface non uniformity. Another explanation may be due to the constant GeI_2:t-butLi that was used for each synthesis. While the concentration of GeI_2 increased the amount of reducing agent remained the same. For the HDA reaction the ratio was as follows: t-butLi:GeI_2 = A) 1:12.7, B) 1:4.2, C) 1:2.5. Although the reducing agent was always in excess it is possible that a decrease in t-butLi could have resulted in more amorphous material and an incomplete reduction of GeI_2.

The last variable studied was the effect of reaction time. As the reaction time was increased from 30 min to 2 hrs the average size of NCs increased as would be expected. A longer time to grow would result in larger particles. Beyond 2 hrs, however, the average NC size was not significantly different from the 2 hr reactions.

The concentration and time effects on a reaction are governed by the Gibbs free energy which is also the driving force behind nucleation and growth. There is a minimum nucleation concentration and a minimum growth concentration. The point at which the minimum growth concentration is less than the minimum nucleation concentration the NCs will stop nucleating and begin to grow by Ostwald ripening. This is why in a colloidal synthesis a fast, single nucleation event is desired so that all the initial NCs are the same size. For growth, a reduction in the Gibbs energy is more desirable for the system. When the GeI_2 is dissolved in the solvent solution the Gibbs

free energy is high. One way for the system to lower its free energy would be to separate the solution into a liquid and solid phase. By introducing a reducing agent into the system, the Ge nanoparticles precipitate out of solution into a separate phase and the total free energy is lowered. This is now a more favorable state for the system than a single phase solution.

The NC growth occurs by the balance of volume and surface free energies. A large NC with low surface energy and high volume energy will either stop or lower its volume energy by the addition of smaller particles. A smaller NC will have a higher surface energy due to the particle having a larger surface to volume ratio. Since surface atoms are more unstable than atoms in the core of the crystal, the smaller particles have a higher surface energy. One way for the NCs to reduce their surface energy is to diffuse and combine with larger particles, which lowers the total free energy of the combined system. This is the principal method for nucleation and growth of NCs in colloidal synthesis. [47]

It should be noted that at longer reaction times for Ge NCs grown in pure HDA the resulting NCs contained less GeO_x as indicated by XRD shown in Figure 10-A.

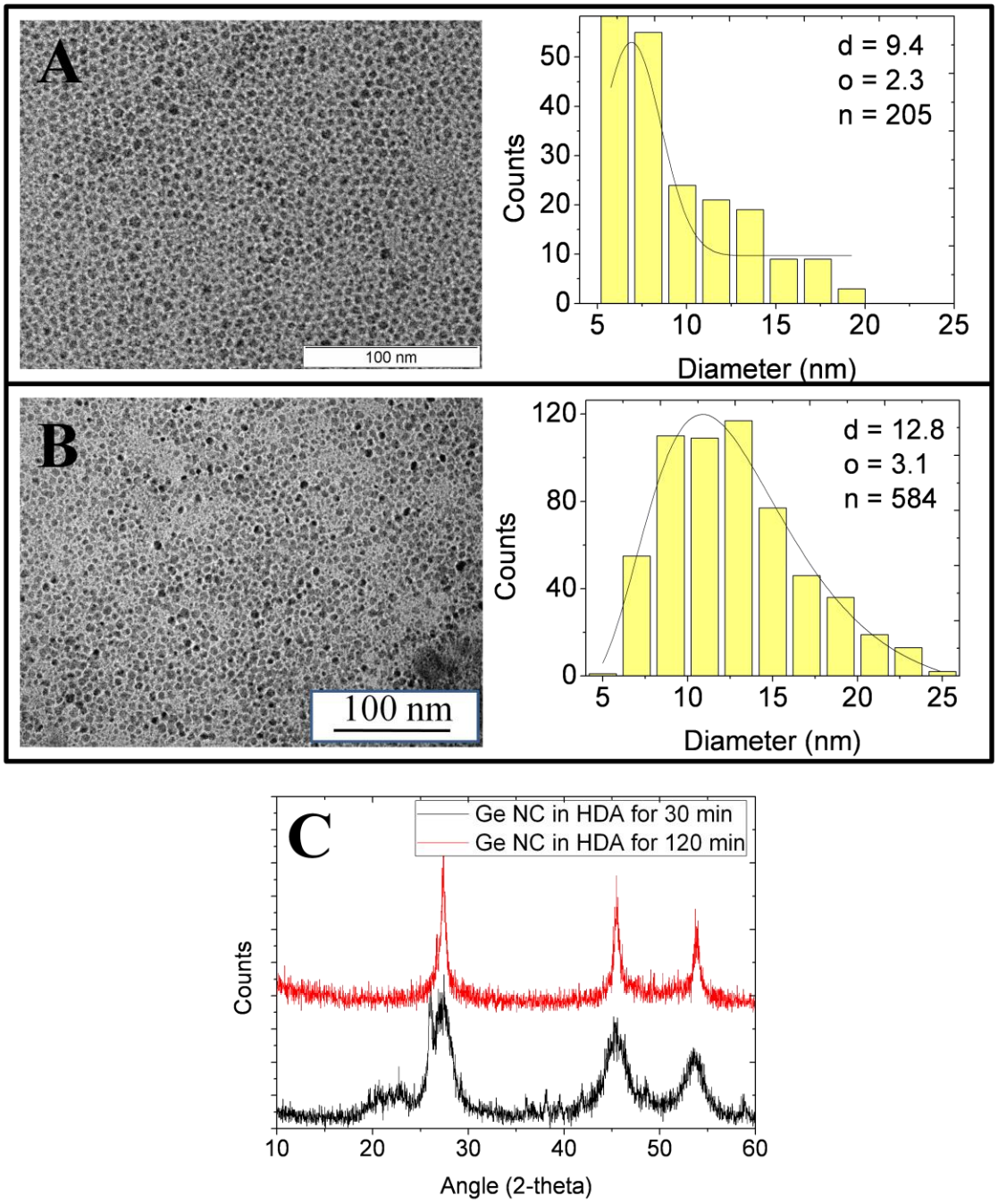

Figure 10**:** A) TEM corresponding to Ge NCs with a reaction time of 30 min (9.4 ± 2.3 nm), B) TEM corresponding to Ge NCs with a reaction time of 120 min (12.8 ± 3.1 nm). (C) (bottom) XRD of Ge NCs from GeI_2 in HDA at 300 °C for 30 min, (top) XRD of Ge NCs from GeI_2 in HDA at 300 °C for 120 min,

There may be two possibilities that attribute to the decrease of GeO_x at longer reaction times. At the initial stages of the reaction there may be oxygen present in the flask. Although the flask is purged with nitrogen there may still be oxygen dissolved in the solution which directly influences the formation of a GeO_x species. As the reaction proceeds, the oxygen could either be liberated from solution or react with the growing Ge. The decrease in the GeO_x content at longer reaction times may be due to a decrease in oxygen concentration in the reaction solution. A 30 min reaction may not be long enough for the final products to stabilize. GeO_x could form at the nucleation step, but over a long enough period of time the GeO_x in solution could be converted to Ge or the oxide layer could be stripped off the particle. Another possibility is that at longer reaction times the final particle solution is more stable in air due to a larger fraction of the particle's surface being covered by the amine ligand. After the reaction is cooled down it is exposed to the atmosphere which normally will oxidize any unprotected particles. A longer reaction time may increase the surface coverage of ligands on the particles surface or increase the stability of the ligand at the particle-ligand interface which would reduce the oxidation of the particles when they are exposed to the atmosphere.

3) *Investigation of Ge NC surface chemistry and related high resolution crystallography.*

The surface composition of three of the seven reactions was analyzed in detail. Although oxidation of Ge NCs shown in XRD scans is a first indication of surface coverage of a ligand, FTIR provides more detail on the types of bonds present. Using FTIR the type of ligand for Ge NCs grown in pure TOP, pure HDA, and a mixture of HDA/ODE were deducted to be a phosphine, an amine, and a carbon ligand,

respectively. This was expected since TOP should provide a phosphine linkage, HDA should provide an amine linkage, and the HDA/ODE reaction should show either an amine or carbon linkage. The indication of Ge-C bond in the FTIR indicated that the affinity of ODE for Ge was stronger than that of HDA and Ge [46]. Figure 11 shows the FTIR of the three types of Ge NCs with different ligands.

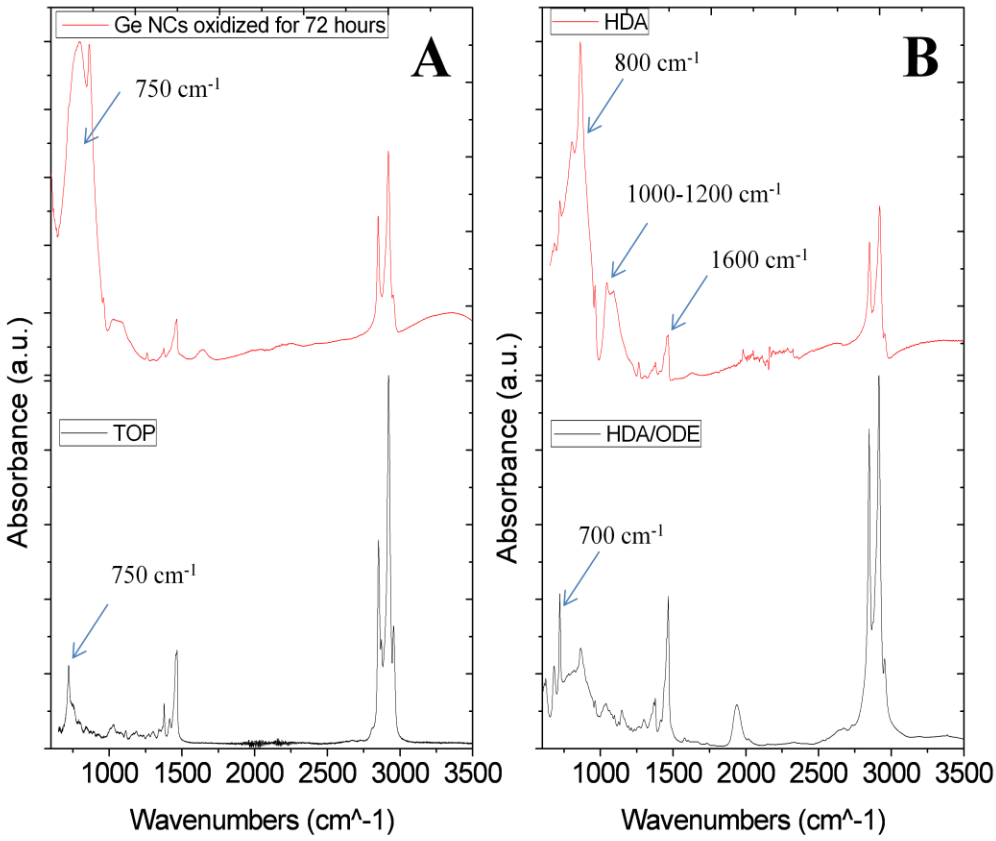

Figure 11: FTIR of Ge NCs grown at 300 °C for 1 hr in A) (bottom) TOP coated Ge NCs and (top) TOP coated Ge NCs from the same sample that has been oxidized for 72 hours, B) (bottom) Ge NCs grown in HDA/ODE and (top) Ge NCs grown in HDA.

From the above figure the small peak at ~1600 cm^{-1}, the medium peak at 1000-1200 cm^{-1}, and the strong peak at 800 cm^{-1} on the HDA sample represent a primary amine. Although the amine could be unwashed HDA from the reaction it is unlikely due to the purity observed in the TEM images and XRD scans. The peak at ~700 cm^{-1} represents a Ge-C bond which is the only distinguishing feature of the Ge NCs grown in HDA/ODE since the ligand is a carbon chain which overlaps with the other common peaks in all samples.

The oxidation of the NCs was also confirmed with the FTIR scans. These showed that HDA coated NCs oxidized faster than ODE coated NCs. This oxidation may have resulted from an incomplete surface coverage during the reaction or poor surface stability. The incomplete surface coverage was confirmed by Figure 11. If the NC density in HDA and HDA/ODE samples was comparable, then there would be a lower C-H stretching intensity in HDA than in HDA/ODE. Since this was not the case, is predicted that the oxidation was due to a lack of surface coverage.

This was confirmed by FTIR in Figure 11. If the NC density in HDA and HDA/ODE samples was comparable, then there would lower C-H stretching intensity in HDA only than in HDA/ODE. Since this was not the case, is predicted that the oxidation was due to a lack of surface coverage.

In addition to FTIR, HR-TEM imaging was done on all three reaction products. These images provided a more detailed understanding of how the crystal lattice was structured. The images also provided more knowledge into whether the functional group in the coordinating solvent was effective for Ge crystal growth. The first of the three samples analyzed was the Ge NCs grown in TOP. Figure 12 shows HR-TEM

images of Ge NCs grown in pure TOP at 300 °C and shows the lattice structure and the defects present.

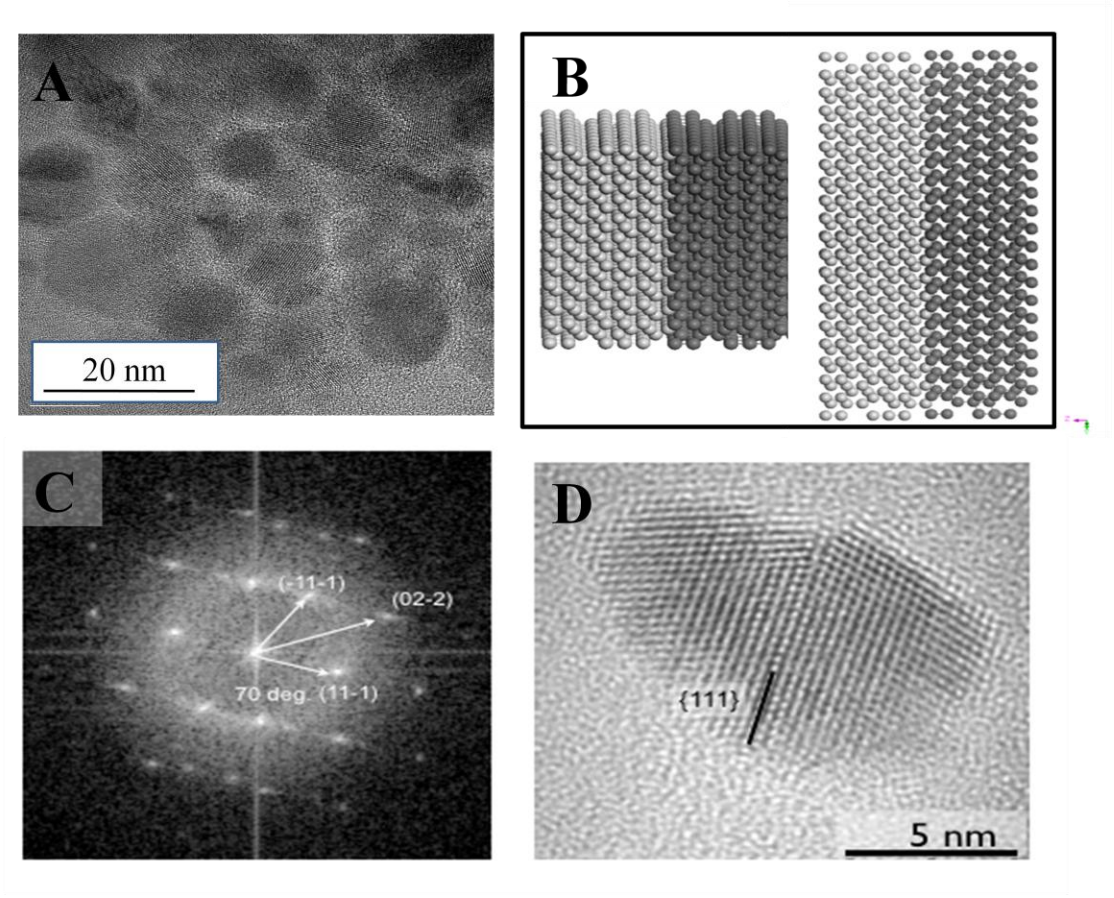

Figure 12: A) HR-TEM of Ge NCs grown in pure TOP at 300 °C for 45 min, B) Twinning model of diamond Ge lattice, C) Diffraction pattern of TEM in A, D) Close-up of a single, 7 nm, Ge NC showing the twinning defect in the (111) plane.

The next two samples analyzed were the reactions where Ge NCs were grown in pure HDA and those grown in a HDA/ODE solution. HR-TEM images of the Ge NCs in pure HDA are shown in Figure 13-A and B. The crystal lattice in these images was analyzed from a sample that was run for 2 hrs at 300 °C. Figure 13-A shows a Ge NC

on its axis. These images also show the FCC structure of the Ge sample with minimal dislocations. The approximate lattice spacing was measured to be ~ 1.5 Å. Figure 13-C shows a HR image of Ge NCs grown in an equal volume of HDA and ODE. The crystal lattice could not be resolved in these images possibly due to the ligand coverage on the particle surface.

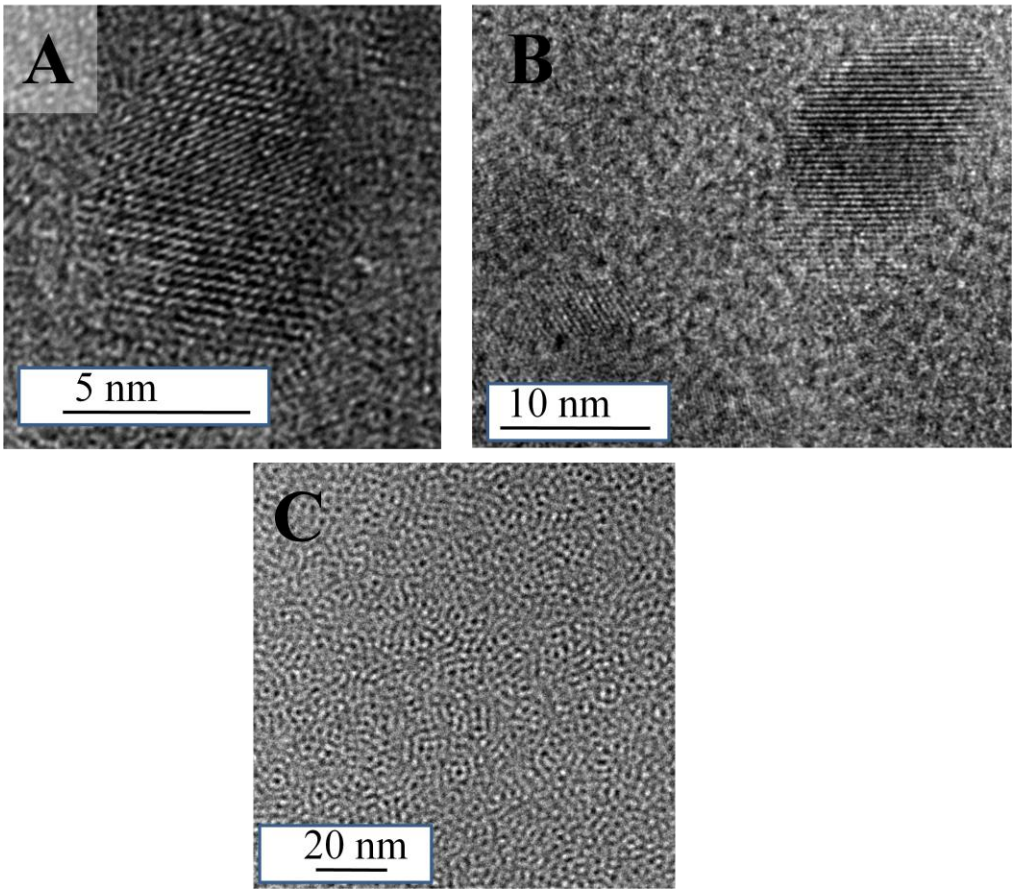

Figure 13: HR-TEM of Ge NC(s) A) grown in pure HDA at 300 °C B) on axis grown in pure HDA at 300 °C. C) grown in an equal volume mixture of HDA/ODE at 300 °C.

4) *Optical properties of the different reactions shown in UV-vis, tauc, and PL plots*

The optical properties of these three samples were also studied using UV-vis spectroscopy. Figure 14 shows the normalized spectrum of the three samples and the change in absorbance onset of the samples.

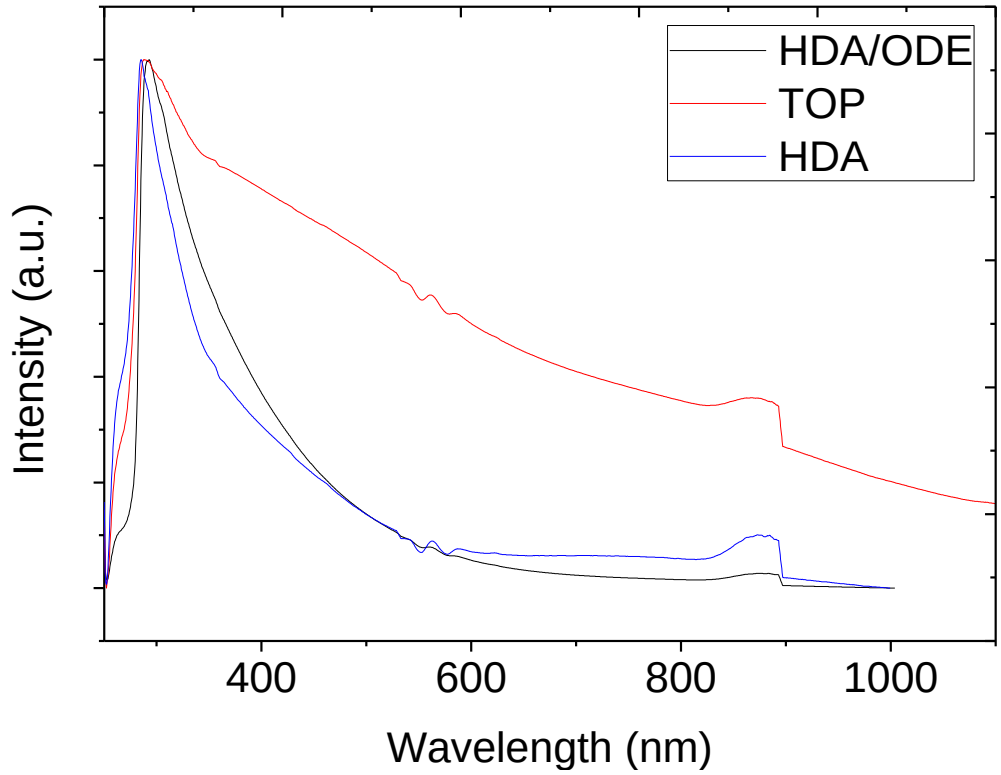

Figure 14**:** UV-vis spectrum of Ge NCs grown at 300 °C for 1 hr in TOP, HDA, and ODE/HDA.

From these spectrums, a tauc plot was constructed to determine the band gap energy which was extrapolated from the slope of a linear fit on each sample. The intersection of the slope with the x-axis gave the E_g. These constructed plots are shown in Figure 15. The E_g were found to be 0.5 eV, 1.4 eV, 1.8 eV, for the TOP, HDA, and ODE coated NCs.

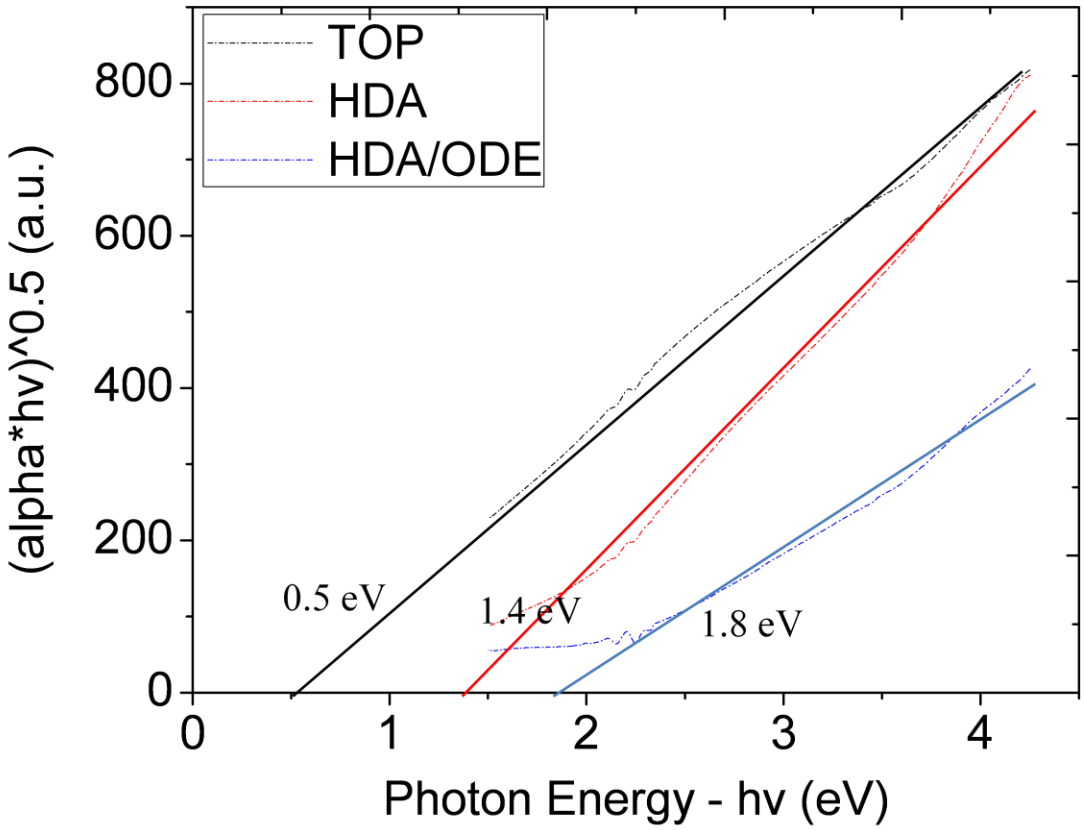

Figure 15: Tauc plot of Ge NCs grown at 300 °C for 1 hr in TOP (12.4 ± 1.8 nm), HDA (4.8 ± 0.8 nm), and ODE/HDA (1.9 ± 0.3 nm).

The band gap energies extracted from Figure 15 indicate the theoretical transition from a direct to an indirect band gap for Ge. Bulk Ge has an indirect band gap of 0.67 eV. As shown in the above figure, as the average NC size becomes smaller as the band gap increases, which was expected. Bulk Ge has a valence band (VB) and conduction band (CB) with the band gap of 0.67 eV between them. As the particle size becomes smaller this gap increases in distance because the energy with which an electron needs to be excited to the CB increases. Approaching the extreme would be a single electron in a NC that would be excited from the VB to the CB that has energy equal to a direct

band gap. This was not experimentally achieved, but the general trend of this effect was illustrated in the tauc plot.

To gain further insight into the size and surface-chemistry dependent optical properties of the Ge nanocrystals, we measured photoluminescence spectra. We compared Ge NCs that were grown in TOP, HDA, and HDA/ODE. The particles grown in HDA/ODE were the only ones that exhibited PL. The PL of these particles had an off center peak with a maximum at ~1025 nm shown in Figure 16.

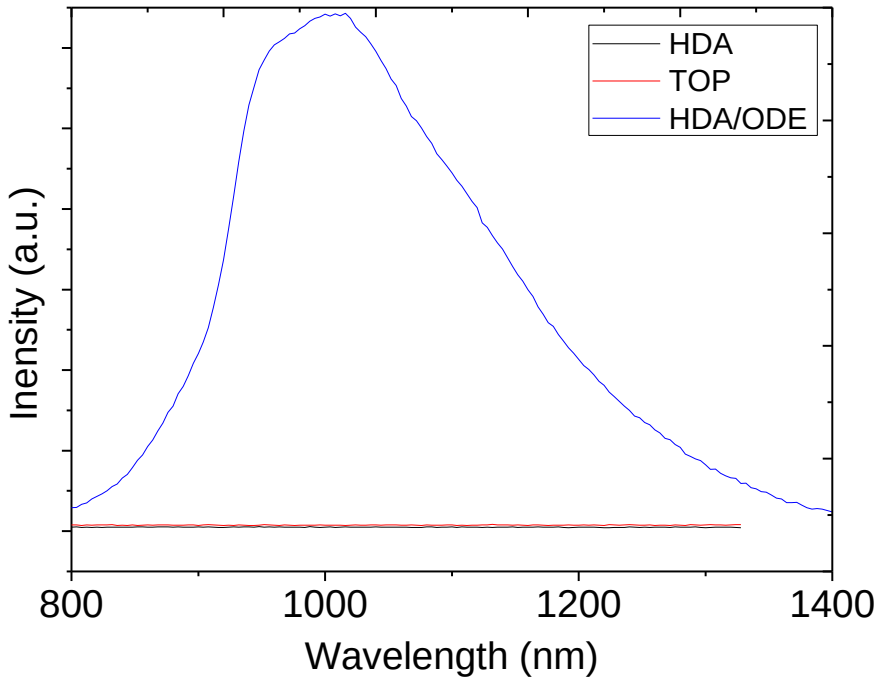

Figure 16**:** PL of ODE capped Ge NCs with a peak at ~1025 nm (1.2 eV).

PL is a recombination event that occurs when the electron becomes excited by a given energy and then returns to its original state giving off light in the form of PL. The presence of PL in the ODE coated Ge NCs indicates that at a given wavelength of light, a fraction of the electrons excited by the electromagnetic spectrum would

recombine and could not be harnessed for electrical energy. The absence of PL that occurs in TOP and HDA coated particles when the electrons in the NC are excited, could be indicative of a trapping of the electrons on the surface of the NC which may be due to ligand effects.

The process by which the electron relaxes to its original state exhibiting PL may either be due to the core or the surface of the Ge NC. It is predicted here that the PL occurred due to the core of the NC. This was hypothesized by the PL and FTIR spectra. The absence of peaks at 1600 cm^{-1} and above 3000 cm^{-1} indicate that the ligand attaches by a 2+2 Diels-Alder-like reaction which can be considered a hyrdogermylation reaction where an alkene is attached to the surface of the NC. The 2+2 reaction results in results in a completely saturated structure. If PL were due to a defective surface then there would be peaks in all samples [46]. The absence of peaks in the TOP and HDA coated particles indicates that the PL was due to the core of the Ge NC.

Applications of Ge nanocrystals

Initial studies of incorporating Ge NCs into a matrix of a-Si was also studied. The Ge NCs were integrated into polycrystalline silicon. This was done by spin coating ~10 nm layer of Ge NCs onto a native oxide Si substrate followed by spin coating a 1:15 CPS:hexane solution. The wafer was then heated for 2 hours at 325 °C to anneal and change the CPS into a-Si. The wafer was laser annealed at different ____ and analyzed using XRD to examine the final crystalline structure. This hybrid device may provide more efficient electron coupling through a photovoltaic device than previous devices. It would also provide a low cost and flexible system if different nanoparticles were

used in the pores of the silicon matrix. The structures of the resulting Si matrices are currently being studied.

Germanium nanowires

Ge nanowires were grown using the supercritical reactor described above. This original method of growth was designed by T. Hanrath and B. Korgel [33]. The method that they developed was a batch process done in a Parr high pressure reactor under the same conditions by which the Ge nanowires were made in this paper. The motivation for synthesizing Ge NWs in a SC fluid is that higher temperatures can be achieved while tuning the fluid propertied better than in a colloidal reaction where a high temperature oily solvent would be needed. The reactor designed for the current work was designed so that a continuous or batch process could be facilitated which allowed for higher quantities of Ge nanowires to be produced and collected in a practical manner. The discussion will be split into two parts; studies done using a batch process and studies done using a plug flow continuous process.

Germanium nanowire batch growth

The effect of temperature, pressure, initial concentration of the Ge precursor and initial concentration of Au nanoparticles in the injected stock solution were studied. All reactions were performed in n-hexane at a pressure of at least 500 psi and a temperature of 380 °C to ensure that the contents of the reactor were in the supercritical regime. Although it may be possible to grow Ge nanowires at an elevated temperature and pressure while not in the supercritical regime the presence of two phases in the reactor during growth would be undesirable. If we choose to run the

reaction at 380 °C but at a lower pressure the hexane would be in the vapor phase. The solubility of a precursor in vapor hexane is significantly lower than that of a supercritical fluid. While the hexane evaporated as it was injected into the reactor, the DPG would be 'left behind' and deposited on the reactor walls before it reached the reactor chamber. This would decrease the concentration of precursor solution during the reaction and ultimately result in low yield syntheses. The contents of the reactor would also not likely be a uniform mixture which would hinder nanowire growth since interactions between Ge and Au particles would be significantly lower than in a supercritical mixture.

Ge NWs grown from this process were analyzed by SEM, EDX, and XRD shown in Figure 17. The Ge NWs were found to be highly crystalline, insoluble in most organic solvents, and had a poor size distribution thought to be due to the large size distribution of Au NCs. The typical product yields for this reaction were ~15%. The XRD scan in Figure 18-D showed a reduction in intensity in the (110) direction which is indicated that the Ge growth along the wire occurred in a layer type growth. This changed the ratio of peaks in the XRD as compared to a sample of Ge nanoparticles with a random crystal orientation. A close-up of a single crystal is shown in Figure 18. These TEM images show the nucleation site of a batch grown Ge NW as well as the oxide that is formed due to air exposure.

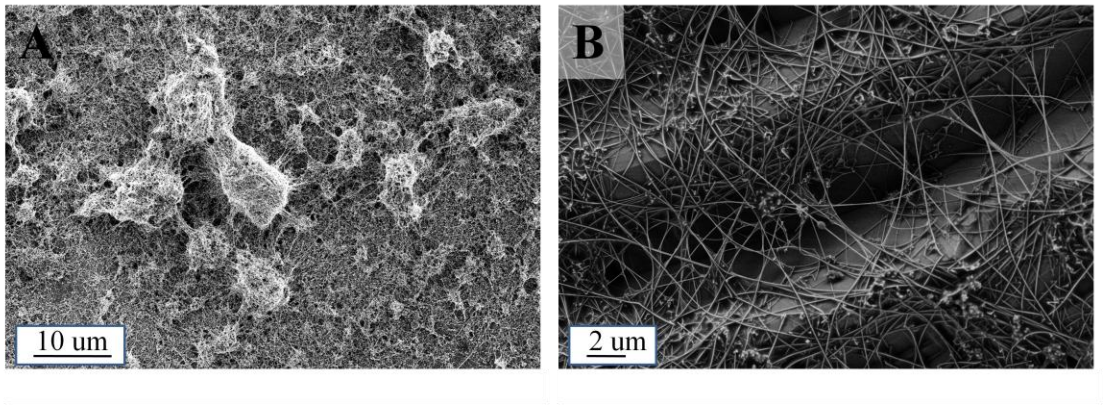

Figure 17: A), B) Ge nanowires grown at 380 C at 1200 psi with a Au:Ge ratio of 1:1200.

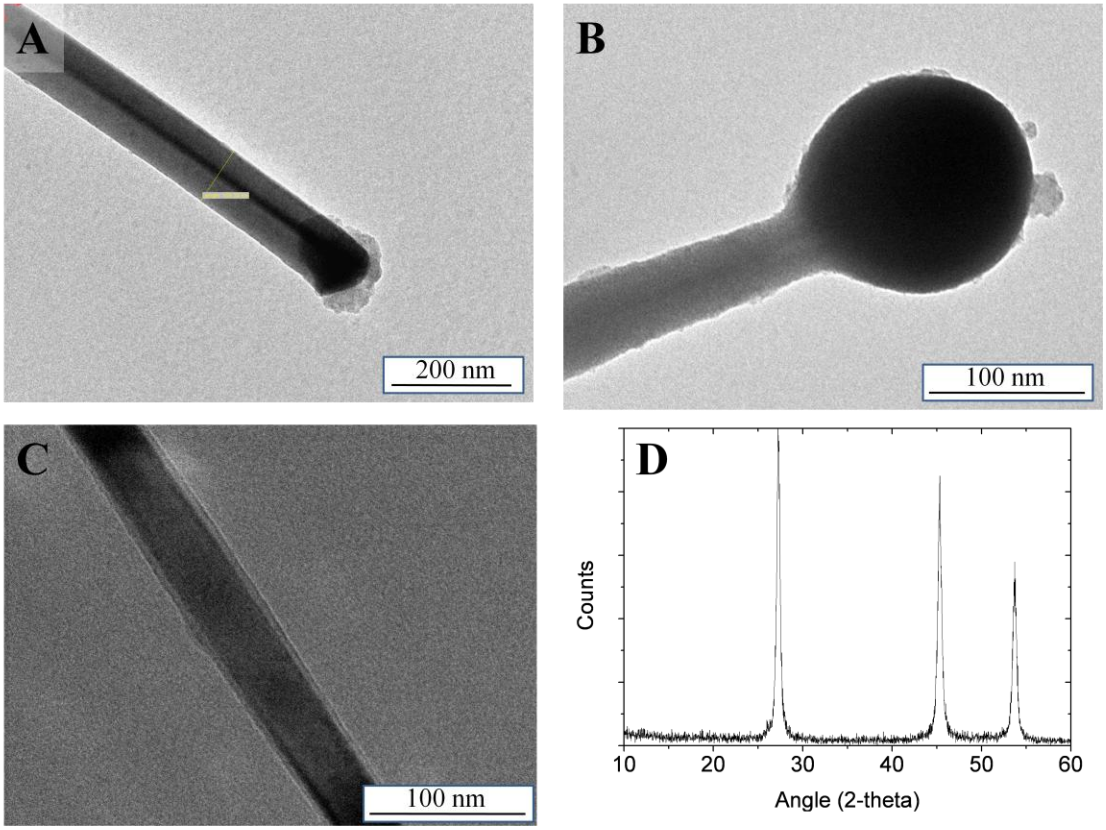

Figure 18: A) Ge NW grown at 380 °C, 1:1200 Au:Ge ratio, 1100 psi (B) 37 nm diameter Ge nanowire at nucleation site (C) 37 nm diameter Ge nanowire with 3 nm oxide layer D) XRD of Ge NWs corresponding to above images.

The Ge NWs were found to be oxygen sensitive as was shown by the thin layer of oxide formed in Figure 18-C. Although this image was taken after 2 hrs of air exposure, XRD showed a large fraction of GeO_x on the NW samples after 3 to 4 hrs. This oxidation indicated that the NWs should be stored under nitrogen or passivated to avoid oxidation.

The first variable studied was the effect of reaction temperature on Ge NW formation. A temperature of 350 °C was required to form any NWs. As the temperature was increased further there was no noticeable difference in the composition of the NW until temperatures above 380 °C. Beyond this temperature NW defects increased and the quality of the NW degraded. The yield was also considerably lower going from a 15 % product yield to a 5% product yield.

The next thing that was studied was the Au:Ge ratio. The ratio of 1:1200 Au:Ge was found to be the optimum mixture that provided the highest yield and quality of wires. A lower ratio lowered the yield which can be explained by a decrease in nucleation sites. An increase of this ratio (>1:1200 Au:Ge) was found to produce the same yield, but NWs of lower quality. This may have been due to an abundance of Au atoms that interfered with growth either by competing homogenous nucleation or unreacted Au that hindered growth and contaminated the final product. Increasing the time the wires were flushed with hexane did not improve the purity of the final product. Figure 19 shows the effects of changing the Au:Ge ratio.

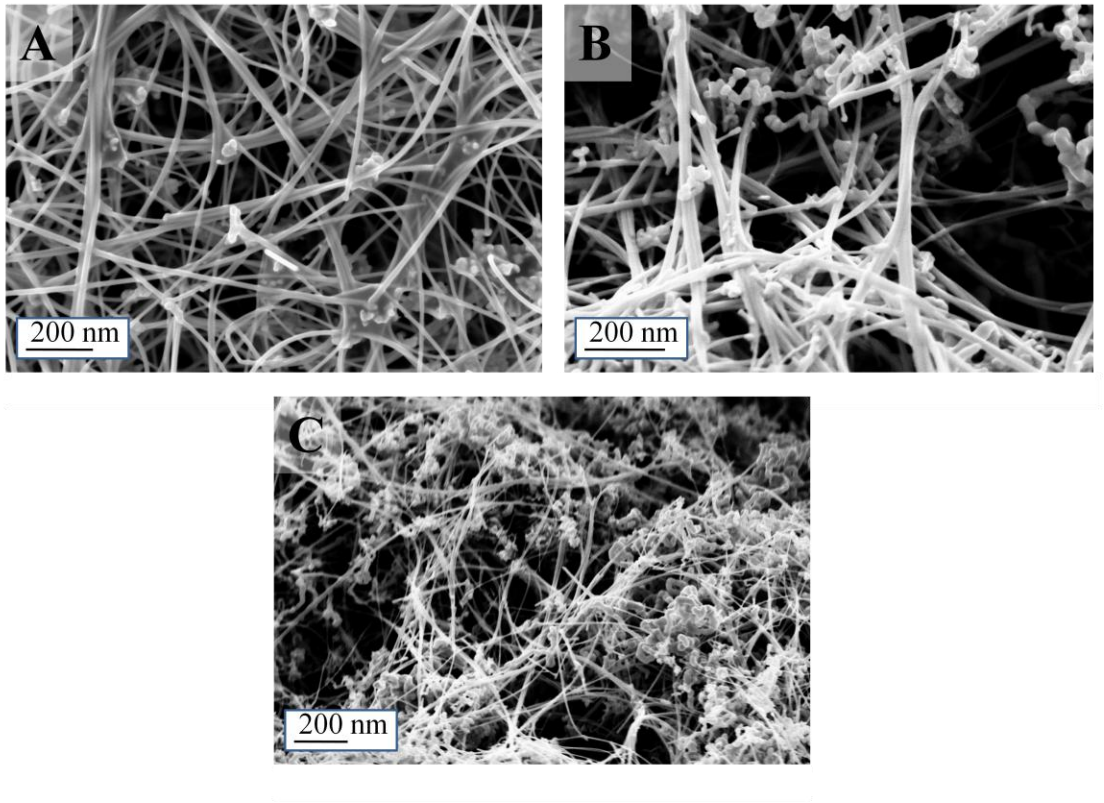

Figure 19: SEM images of Ge NWs at a constant temperature of 380 °C and a pressure of 1100 psi using a Au:Ge ratio of A) 1:1200, B) 1:800, and C) 1:500.

In the total absence of a seed crystal and at higher temperatures Ge NWs do not form, but rather NCs. Ge NCs were also synthesized in the supercritical reactor by the thermal decomposition of DPG. This reaction was as carried out in an attempt to synthesize Ge NCs with a narrow, well defined size distribution than could be achieved in the colloidal synthesis. It also provided a contrast to colloidally grown Ge NCs with ones grown by thermal degradation. A 1:9 ratio DPG to hexane was injected into the reactor where the solution was allowed to react for 10 min at 450 °C and 2000 psi. The yellow, oily solution containing particles was collected from the reactor. This solution was analyzed using TEM shown in Figure 20. The oily residue was a result of the decomposition of the n-hexane to yield organic byproducts. Vacuum drying and

precipitation of the particles removed most of the unwanted byproduct, but the yield (~5%) could not be improved so this method was not studied further.

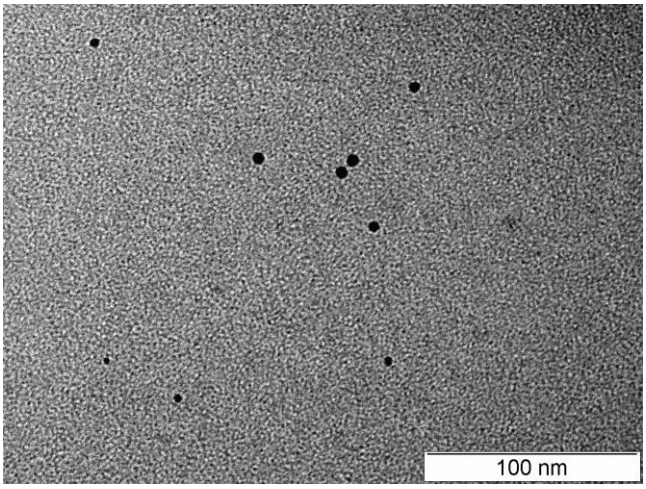

Figure 20: (A) TEM of ~ 7 nm Ge particles synthesized in SC hexane at 450 °C and 2000 psi for 10 min.

The last variable that was studied was the density of the fluid in the reactor which was studied by changing the pressure using the inlet pump for the reaction. Pressures from 500 psi to 2000 psi were studied. As 500 psi the reaction yielded a low yield of NWs which may have been due to a lack of particle interactions and nucleation events. As the pressure was increased to 1200 psi the yield improved as did the quality of the NWs. At a higher pressure of 2000 psi the product yield started to decrease, the crystal growth defects increased, and Ge NCs started to form in small quantities.

Supercritical Ge NW growth was also attempted by substituting TMG for DPG which has a lower degradation temperature. The reaction conditions were similar to the reactions done with DPG (i.e. 350 °C, 1100 psi, and a 1:1200 Au:Ge ratio). This

reaction had little success in that the small yield of final product was always contaminated with unreacted materials. The low yield, impure Ge NWs could not be resolved with an SEM. Although initial attempts were unsuccessful with TMG, further studies of initial concentration and temperature may prove promising.

Another variation of Ge NW growth used Bi as a substitute for Au in attempts to provide an alternative seeding crystal. These reactions were also unsuccessful and did not produce Ge NWs. The final products examined with TEM showed mostly organic materials. The purpose of substituting Bi was to study how a material with a lower melting point interacted with DPG. The lower eutectic temperature would provide a method to synthesize Ge NWs at lower temperatures, which would require less energy to grow Ge NWs, an important practical issue to consider for scale up processes.

Continuous growth

Figure 2 depicts the process and experimental setup for a semi-continuous Ge nanowire procedure. The system is flushed with hexane, pressurized, and heated to the desired operating temperature. The feed solution is pumped at a steady flow rate. The system insures a steady state flow by utilizing a pressure relief valve. This valve is field adjustable and will enable a constant flow through the steady state system for the duration of the experiment. Once the system is in steady state, the prepared reaction feed solution is introduced into the system. The wires were collected in the collection vessel while the byproducts and reacted liquid were continuously flushed through the system. With the flow through system, in absence of NWs attaching to the surface of the reactor chamber, a large fraction of the NWs can be continuously collected.

Although this was achieved with the current design, higher fractions of the NWs could likely be collected with a different material such as titanium.

When the process is complete, the flow-through stream is switched to another collection flask. The wires can either be collected by rapidly depressurizing the system and collecting the wires that come out of the system or slowly lowering the pressure and collecting the wires from the collection chamber. The rapid decrease in pressure often clogs the smaller tubing, making it difficult to collect all the Ge wires. Collecting the wires from the chamber after slowly depressurizing the system, however, was time consuming because the system must be disassembled.

Continuous Ge nanowire growth via thermal decomposition of DPG in the presence of Au has been done at a pressure of 1100 psi and a limiting temperature of 380 °C. Higher temperatures were not attempted with the current stainless steel material to remain below the recommended operating safety parameters. The initial reaction feed solution was a 1:1200 Au:Ge ratio diluted with 15 mL hexane. A 200 mM DPG concentration was used for all reactions. The reactor was flushed with n-hexane after the synthesis to rinse the nanowires of any unreacted DPG or byproducts from the reaction. Product yields of up to 40% (100 mg quantities) were achieved or ~10 mg/min.

The effect of changing the flow rate of the system was the main variable studied to determine its effects on Ge NW growth. SEM images in Figure 21 show the effects of increasing the flow rate from 1.3 mL/min to 3.0 mL/min. The reactor volume was changed for each flow rate to achieve a 10 minute residence time. The purity of the

sample was confirmed by EDX which showed only Ge, slight traces of oxygen, and the Si background.

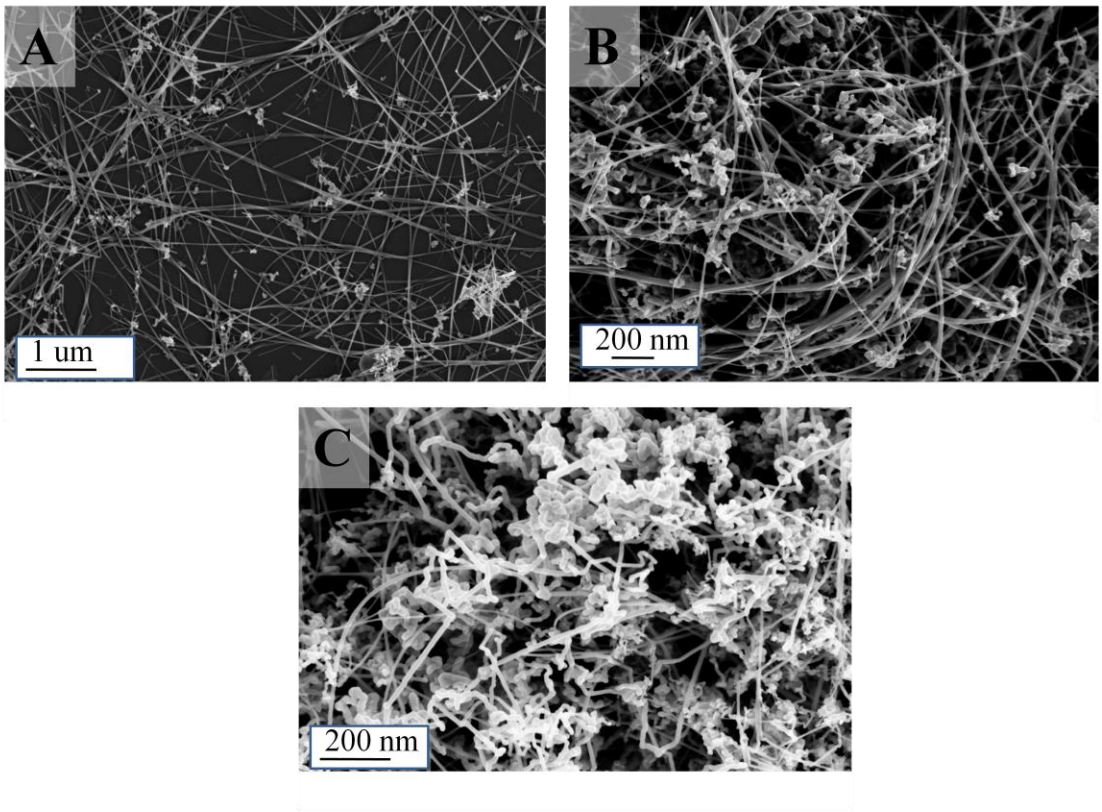

Figure 21**:** SEM images of Ge NWs at 380 °C, 1100 psi, residence time = 10 min for a continuous reaction with a flow rate of (A) 1.3 mL/min (B) 2.0 mL/min (C) 3.0 mL/min.

These images show that as the flow rate is increased above 2.0 ml/min the defects in growth of the NWs become significant. Above this flow rate there were numerous kinks and 'mangled nanowires' formed. The reason behind this is thought to be to the increase in disturbances, while still remaining in a laminar flow regime, during the growth phase. Higher flow rates may produce more disturbances, wire-wire interactions, and friction against the substrate and reaction walls that would prohibit

the growth of a near perfect nanowire as would occur if the nanowire were suspended in the reactor during a batch process. The defects would also increase if there is an overwhelming affects of the seed growth or if the growth becomes so fast that epitaxial growth cannot be maintained. Below 2.0 mL/min however the defects in the wires was greatly reduced.

It should also be noted that both in this process as well as in the batch reactions the wires typically had a wide diameter size distribution (± 30% average deviation from avg. size). This was thought to originate from the wide size distribution of Au nanoparticles which ranged from 2 - 10 nm. Since the nucleation of the wire begins at a Ge:Au droplet, various sizes of this droplet would result in different wire diameters. Another issue to consider with this process is that with a stainless steel material there is a small fraction of wires that stick to the reactor walls which continue to grow while others flow through. It is predicted that another reactor material such as titanium, or a high temperature grade polymer coating, may solve this wire adhesion during the synthesis.

Preliminary depositions of Au, PbSe, and Ge nanoparticles in hexane were studied for their potential applications in photovoltaics. Each nanoparticle solution was drop cast onto a dilute mesh of Ge NWs. The composition of the resulting structures is shown in Figure 22.

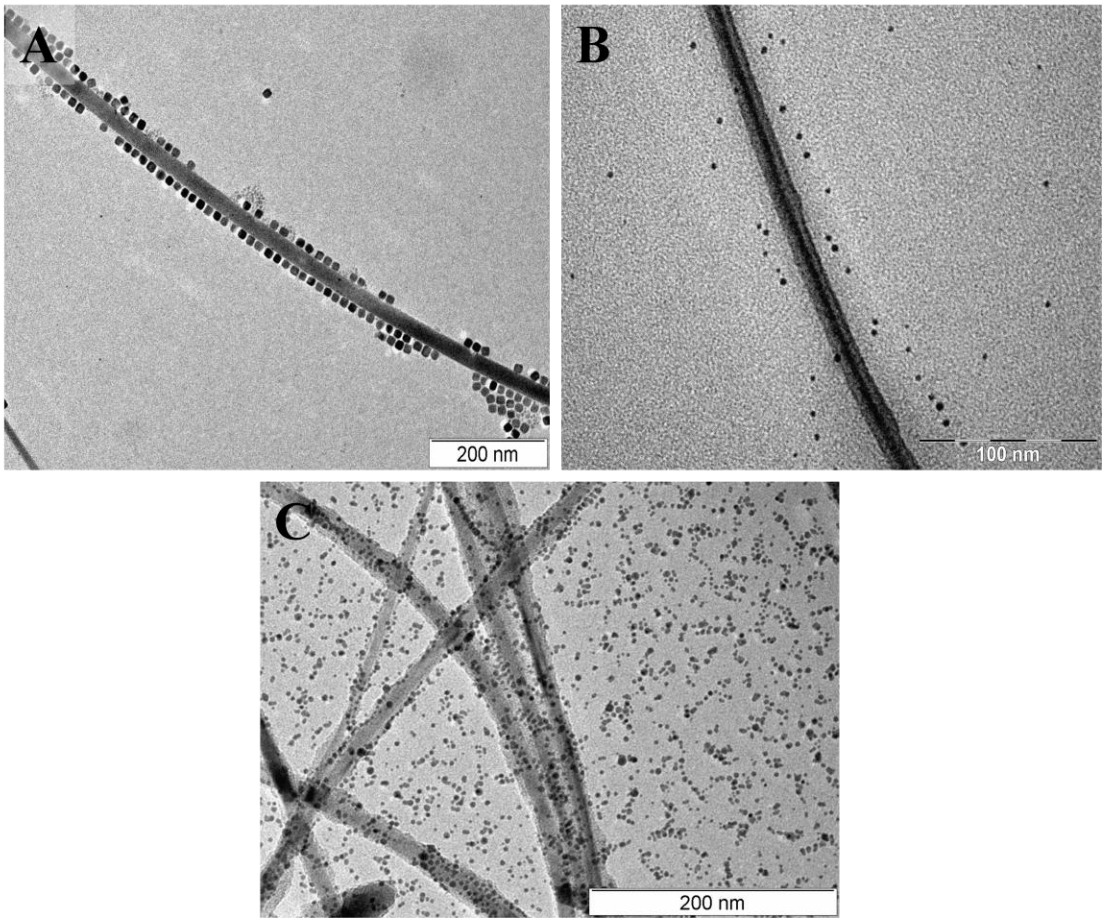

Figure 22: A) Ge NW with PbSe nanoparticles physisorbed to surface B) Ge NW with Ge nanoparticles physisorbed to surface C) Ge NW with Au nanoparticles physisorbed to surface of the NW.

The purpose of this experiment was to study how particles adhere to the surface of the NW surface. On a 2 dimensional surface, as simulated with a TEM grid, the particles are attracted to the surface of the wire by Van der Walls attractions. The ligand on the surface of the NC influences the particle-particles, particle-wire interactions as well as the distance between the other particles and the surface of the NW.

The benefit of an all inorganic heterojunction solar cell of NCs coating NWs would facilitate charge transport. Theoretically the quantum confinement effects of the NC, which would allow a photon with given energy to create an electron-hole, would occur in the NC. Once a photon creates a charge separation the charge would be transferred to the NW. This would aid in charge separation because the NWs act as a 1 dimensional charge transferring structure [48]. This would reduce the recombination rate and increase the efficiency of the solar cell by transferring the charges more effectively to the electrode.

FUTURE WORK

A few challenges that must be overcome in order to effectively work with Ge nanomaterials are the issues of oxidation and ligand exchanges. Currently the only oxygen resistant material is ODE capped Ge NCs. The problem with these NCs is that the Ge-C bond is too strong to remove by standard ligand exchanges, which restricts the surface studies that can be done and limits the interparticle spacing due to the length of the ligand shell. TOP coated particles, shown to oxidize more readily than ODE coated particles, may be more suitable for modifying their surfaces to accommodate ligands that would be more desirable for device applications.

Another issue to consider is the oxidation of the Ge NWs. To effectively work with these materials the wire surfaces should be modified to provide a layer of protection against oxidation. Some studies have been done to solve this issue by introducing a ligand during the SC synthesis [49]. In the current continuous system a proposed solution would be to add a passivating solvent in the collection chamber so that as the NWs are deposited in the chamber, still at high temperature and pressure, they would be in contact with and potentially coated with a passivating ligand. This would still allow the process to be completed in a single step synthesis and protecting the wires from oxidation.

Once these challenges are overcome the next step in this project is to apply the Ge NCs and Ge NWs to fabricating photovoltaic devices and to study the fundamental device interfacial properties and charge recombination and their relation to the photovoltaic performance of these materials. From these studies and a better understanding and control of interfacial properties, prototype photovoltaic devices can be engineered to maximize the overall photon conversion efficiency. These materials

will be important for a variety of next generation photovoltaic layouts. The particles will be important for integrated heterojunctions while the nanowires can be used for nanowire/nanoparticle hybrids.

Once the photovoltaic devices are assembled the interface and surfaces of the materials at the active layer edges in photovoltaic devices can be characterized. The thermodynamics and kinetics at the interface will be applied to study these properties. Specifically for Ge nanoparticles, the particles will be drop or spin cast onto a substrate and the effects of interparticle spacing will be studied by reducing the distance between each particle, possibly using hydrazine or another replacement ligand [50]. This process as well as the types of ligands that are compatible to replace the current TOP and ODE coated particles is currently being studied. The conflicting parameters of increased conductivity and the stability of the composition of the film as the interparticle spacing is reduced will be studied. The Ge nanowires will be prepared for device application by shortening them to a uniform length, possibly by sonicating, and studying how the wires orient under an electric field. Initial studies have been done to align the Ge NWs under a magnetic field shown in Figure 23. In depth characterization of electron transport in Ge arrays and heterostructures will then be performed to better understand how to assemble efficient and practical solar cells.

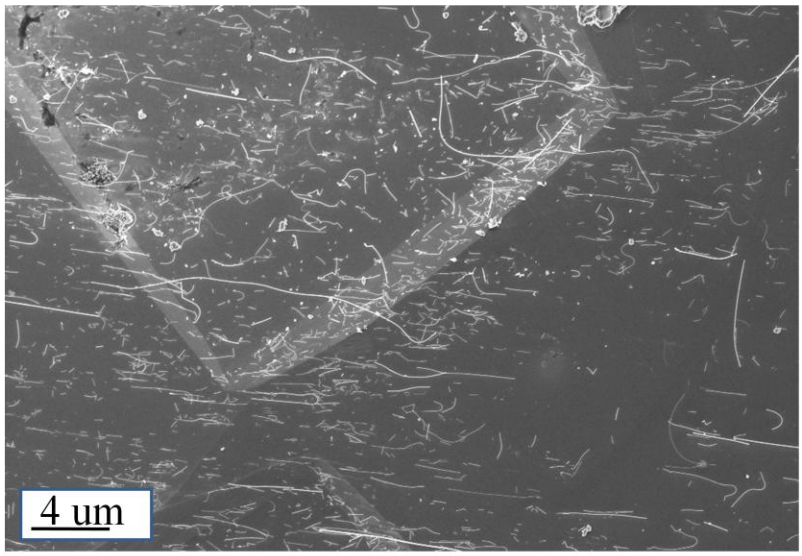

Figure 23: Ge NWs that were dropcast onto a Si substrate in the presence of a magnetic field.

There are possible two active layers for devices that can be fabricated form the synthesized Ge nanomaterials. The first active layer would use PbSe or Ge NCs that are physisorbed onto Ge wire surfaces between a layer of indium titanium oxide and Al. Charge transfer can then be measured via photoinduced absorbance spectroscopy or scanning photocurrent spectroscopy. The second device idea is an all inorganic heterojunction solar cell. The PbSe or Ge nanoparticles could be integrated into polycrystalline silicon. The polycrystalline silicon would be formed either from heating a mixture of spin coated CPS and Ge on a Si wafer and then exposing it to UV light or through a-Si deposition on a thin film of Ge NCs. To better illustrate this device, Ge NCs were spun cast onto a Si substrate before the a-Si was deposited shown in Figure 24.

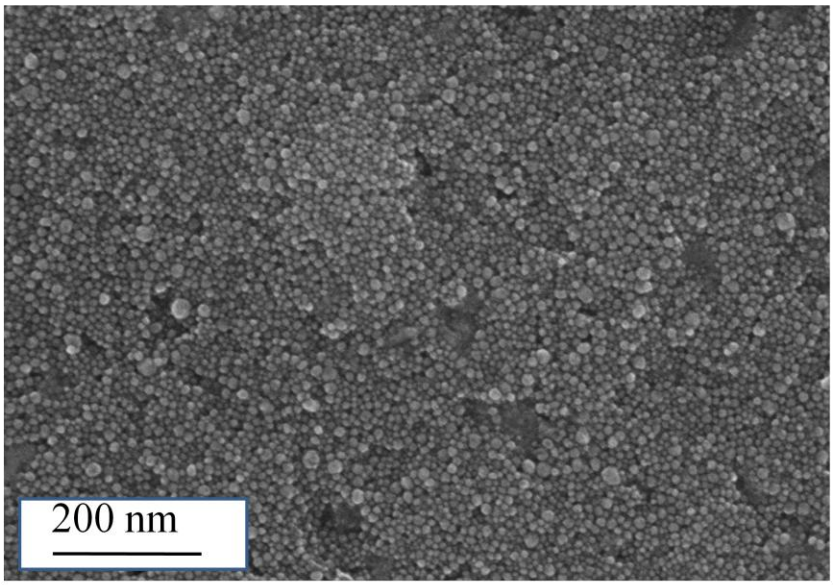

Figure 24: SEM image of Ge NCs spin coated onto Si substrate prior to a-Si deposition.

This Figure shows that the synthesized Ge NCs are abundant enough to sufficiently coat the surface, but research must still be done to explore the best method of uniformly coating the Ge NCs. Once a semi-uniform thin film of Ge is deposited a-Si will be deposited onto the surface either by sputtering or CPS. The matrix material is predicted provide faster and more efficient electron coupling through the cell than previous devices [51]. It would also provide a low cost and flexible system if different nanoparticles were used in the pores of the silicon matrix.

CONCLUSION

Ge NCs were synthesized via a number of different colloidal syntheses. Two reliable synthetic approaches have been found using GeI_2 as a precursor with the strong reducing agent, tert-butyllithium. The first reaction was performed in pure TOP which served as the solution solvent as well as the stabilizing ligand. These particles were 10 – 12 nm in size and were resistant to oxidation up to 6 hours in air, but could be stabilized under a nitrogen atmosphere for over 6 months. These particles did not luminescence. The second reaction was in an equal volume mixture of ODE and HDA yielding 1.9 ± 0.3 nm particles that showed PL at ~1025 nm. These particles were resistant to oxidation up 24 hours in air, but were more difficult to extract from the reaction. In all reactions in was found that a minimum temperature of 250 °C was required to crystallize the nanoparticles. Through imaging using HR-TEM the Top coated Ge NCs were found to have numerous twinning in the crystal structure. This indicated that unlike PbSe or CdSe nanoparticles Ge is more difficult to crystallize which resulted in high occurrence of crystal defects.

In addition to synthesizing Ge nanocrystals a continuous process to grow Ge nanowires was designed and implemented. This process was developed to provide a method for a practical large scale production of nanowires. Although an increase in flow rate was shown to increase crystal defects, below 2.0 mL/min yielded high quality Ge nanowires with a low defect rate at 40% product yields.

REFERENCES

1. Crabtree, G.W. and N. Lewis, *Solar energy conversion.* Science, 2007: p. 37-42.
2. Mayes, F. and L. Guey-Lee, *Renewable Energy Trends in Consumption and Electricity, 2005*, U.S.D.o. Energy, Editor. 2005, Energy Information Administration: Washington, DC.
3. Lewis, N., *Chemical Control of Charge Transfer and Recombination at Semiconductor Photoelectrode Surfaces.* Inorg. Chem., 2005. **44**: p. 6900-6911.
4. Shockley, W. and H.J. Queisser, *Detailed Balance Limit of Efficiency of P-N Junction Solar Cells.* Journal of Applied Physics, 1961. **32**(3): p. 510-&.
5. Nelson, J., *The Physics of Solar Cells*. 2003, London: Imperial College Press.
6. Nozik, A.J., *Multiple exciton generation in semiconductor quantum dots.* Chemical Physical Letters, 2008. **457**: p. 3-11.
7. Allen Barnett, et al., *Initial test bed for very high efficiency solar cells.* 2007.
8. Green, M.A. and S.R. Wenham, *Novel Parallel Multijunction Solar-Cell.* Applied Physics Letters, 1994. **65**(23): p. 2907-2909.
9. Heath, J.R., J.J. Shiang, and A.P. Alivisatos, *Germanium quantum dots: optical properties and synthesis.* Journal of Chemical Physics, 1994. **101**(2): p. 1607-15.
10. Warner, J.H. and R.D. Tilley, *Synthesis of water-soluble photoluminescent germanium nanocrystals.* Nanotechnology, 2006. **17**: p. 3745-3749.
11. Zhou Z, B.L.a.F.R., Nano Lett, 2003(3): p. 163.
12. Werner, J.H., S. Kolodinski, and H.J. Queisser, *Novel Optimization Principles and Efficiency Limits for Semiconductor Solar-Cells.* Physical Review Letters, 1994. **72**(24): p. 3851-3854.

13. Mentzel, T.S., et al., *Charge transport in PbSe nanocrystal arrays.* Physical Review B, 2008. **77**.
14. Heath, J.R., Science, 1992. **258**: p. 1131.
15. Taylor, B.R., et al., *Solution synthesis and characterization of quantum confined Ge nanoparticles.* Chem. Mater., 1999. **11**: p. 2493.
16. Wilcoxon, J.P., P.P. Provenico, and G.A. Samara, *Synthesis and optical properties of colloidal germanium nanocrystals.* Phys. Rev. B, 2001. **64**: p. 035417-1.
17. Wang, W., et al., *Synthesis of gram-scale germanium nanocrystals by a low-temperature inverse micelle solvothermal route.* Nanotechnology, 2005. **16**: p. 1126-1129.
18. Iacona, F., G. Franzo, and S. C., *Correlation between luminescence and structural properties of Si nanocrystals.* J. Appl. Phys., 2000. **87**: p. 1295-1303.
19. G. Chen, M.S.D., J.-P. Fleurial, T. Caillat, Int. Mater. Rev., 2003. **48**: p. 45.
20. Chan, C.K., X.F. Zhang, and Y. Cui, *High Capacity Li Ion Battery Anodes Using Ge Nanowires.* Nano Letters, 2008. **8**: p. 307.
21. Chan, C.K., et al., *High-performance lithium battery anodes using silicon nanowires.* Nature Nanotechnology, 2008. **3**: p. 31-35.
22. Loscutoff, P.W. and S.F. Bent, *Reactivity of the Germanium Surface: Chemical Passivation and Functionalization.* Annual Review of Physical Chemistry, 2006. **57**: p. 467-495.
23. Alguno, A., et al., *Enhanced quantum efficiency of solar cells with self-assembled Ge dots stacked in multilayer structure.* Applied Physics Letters, 2003. **83**(6).

24. Lu, X., et al., *Synthesis of Germanium Nanocrystals in High Temperature Supercritical Fluid Solvents.* Nano Letters, 2004. **4**(5): p. 969-974.

25. Zaitseva, N., et al., *Germanium Nanocrystals Synthesized in High-Boiling-Point Organic Solvents.* Chem. Mater., 2007. **19**: p. 5174-5178.

26. Heath, J.R., J.J. Shiang, and A.P. Alivisatos, *Germanium Quantum Dots - Optical-Properties and Synthesis.* Journal of Chemical Physics, 1994. **101**(2): p. 1607-1615.

27. Gerion, D., et al., *Solution Synthesis of Germanium Nanocrystals: Success and Open Challenges.* Nano Letters, 2004. **4**(4): p. 597-602.

28. Lu, X.M., B.A. Korgel, and K.P. Johnston, *Synthesis of germanium nanocrystals in high temperature supercritical CO2.* Nanotechnology, 2005. **16**(7): p. S389-S394.

29. Wu, H.P.G., M. Y.; Yao, C. W.; Wang, Y. W.; Zeng, Y. W.; Wang, and G.Q.J. L. N.; Zhang, J. Z., Nanotechnology, 2006. **17**: p. 5339-5343.

30. Lu, X.M., B.A. Korgel, and K.P. Johnston, *High yield of germanium nanocrystals synthesized from germanium diiodide in solution.* Chemistry of Materials, 2005. **17**(25): p. 6479-6485.

31. Tao, A.R., S. Habas, and P. Yang, *Shape Control of Colloidal Metal Nanocrystals.* Small, 2008. **4**(3): p. 310-325.

32. Murray, C.B., et al., *Colloidal synthesis of nanocrystals and nanocrystal superlattices.* Ibm Journal of Research and Development, 2001. **45**(1): p. 47-56.

33. Hanrath, T., *Germanium Nanowires: Synthesis, Characterization, and Utilization*, in *Chemical Engineering*. 2004, University of Texas at Austin: Austin.

34. Hanrath, T., *Germanium Nanowires: Synthesis, Characterization, and Utilization.* 2004.

35. Hanrath, T., *Crystallography and Surface Faceting of Germanium Nanowires.* Small, 2005. **7**: p. 717-721.

36. Tuan, H.Y., et al., *Germanium nanowire synthesis: An example of solid-phase seeded growth with nickel nanocrystals.* Chemistry of Materials, 2005. **17**(23): p. 5705-5711.

37. Tuan, H.-Y., *Synthesis and Characterization of Silicon and Germanium Nanowires, Silica Nanotubes, and Germanium Telluride/Tellurium Nanostructures.* 2007.

38. LT, N., A. D, and e.a. Sader JE, *Ultimate-Strength Germanium Nanowires.* Nano Letters, 2006. **6**(12): p. 2964-2968.

39. C. Miesner, K.B., and G. Abstreiter, *Lateral photodectors with Ge quantum dots in Si.* Infrared Physics and Technology, 2001. **42**: p. 461-465.

40. Zhou, P., et al., *Fabrication, structure and magnetic properties of highly ordered prussian blue nanowire arrays.* Nanoletters, 2002. **8**(2): p. 845.

41. Green and Wenham, *Novel parallel multijunction solar cell.* Appl. Phys. Lett., 1994. **65**(23): p. 2907-2909.

42. Milliron, D.J., I. Gur, and A.P. Alivisatos, *Hybrid organic - Nanocrystal solar cells.* MRS Bulletin, 2005. **30**(1): p. 41-44.

43. Brust, M., et al., *Synthesis of thiol-derivatized gold nanoparticles in a two-phase liquid-liquid system.* Journal of the Chemical Society, Chemical Communications, 1994(7): p. 801-2.

44. Tauc, R.G., A. Vancu, Phys. Stat. Sol., 1966. **627**.

45. Paul W. Loscutoff, S.B., *Reactivity of the Germanium Surface.* Phys. Chem., 2006. **57**: p. 467-495.

46. Doh C. Lee, J.M.P., Istvan Robel, Donald J. Werder, Richard D. Schaller, and and V.I. Klimov, *Colloidal Synthesis of Infrared-Emitting Germanium Nanocrystals.* J. Am. Chem. Soc., 2008(131): p. 3436–3437.

47. Rich Robinson, T.H. 2008.

48. Shah, P.S., et al., *Nanocrystal and nanowire synthesis and dispersibility in supercritical fluids.* Journal of Physical Chemistry B, 2004. **108**(28): p. 9574-9587.

49. Hanrath, T. and B.A. Korgel, *Chemical surface passivation of Ge nanowires.* J. Am. Chem. Soc., 2004. **126**: p. 15466-15472.

50. Talapin, D.V. and C.B. Murray, *PbSe Nanocrystal Solids for n- and p-Channel Thin Film Field-Effect Transistors.* Science, 2005. **310**(5745): p. 86-89.

51. Hanrath, T. 2009.